

SURMOF Induced Polymorphism and Crystal Morphological Engineering of the Acetaminophen Polymorphs: Advantage of heterogeneous nucleation

Geetha Bolla and Allan. S. Myerson*

Department of Chemical Engineering, Massachusetts Institute of Technology, 77 Massachusetts Avenue, E19-502b, Cambridge, Massachusetts 02139, United States

Experimental Section

Materials, methods: Acetaminophen, 12-Mercaptododecanoic acid, Cupper acetate hydrate and Trimesic acid were purchased from Sigma-Aldrich (St. Louis, MO) and used as received. Ethanol (HPLC grade) was purchased from VWR International (Edison, NJ). Gold substrates purchased from Evaporated Metal Films Corp, EMF Ithaca, Ithaca, NY 14850. Crystallization of the APAP from EtOH solvents to check the morphology. For the SURMOF analysis solutions were prepared 1mg/mL to 10mg/mL and liquid phase epitaxy dipping and drop casting methods.

Preparation of HKUST-1 MOF: A mixture of $\text{Cu}(\text{OAc})_2 \cdot \text{H}_2\text{O}$, 1.5 equiv. with respect to Trimesic acid H3BTC in DMF was added, and the mixture was stirred at 110 °C for 12 hrs. The resulting suspension was cooled, then the solid was filtered through gravity filtration and overnight dried at 70-80 °C.

Preparation of the self-assemble monolayers: The substrate coated with 5 nm titanium layer and a 10 nm gold layer was cleaned by immersing the substrates in acetone for 2 h and dried under nitrogen gas. Fabricated substrates mentioned above were cleaned with piranha solution (a typical mixture of 3:1 concentrated sulfuric acid to 30% hydrogen peroxide solution) for 20 min for the cleaning of all organic impurities from the surface. Substrates were then washed with copious amounts of pure water by sonication about 10-15 min and further the same with isopropanol, then dried with a nitrogen gun. Now the substrates were ready to prepare for self-assembled monolayers (SAMs). Monolayer preparation was carried out, gold substrates were kept in the 10 mmol thiol, 12-Mercaptododecanoic acid (12-COOH) solution for 18 h and further washed with ethanol, IPA and blown dry by a jet of nitrogen.

Preparation of the SURMOFs: Prepared SAM substrates were dipped very slowly to the 10 mmol metal and ligand source solution in EtOH solvent with container as beakers at room temperature 22 °C. Each time and step we have done washing with solvent to make more clean surface and removed excess metal or ligand on surface. The total process named as Layer by Layer Dipping (LBL-D).

Growing Single Crystals of APAP polymorphs on SURMOF: Crystallization experiments were performed pure EtOH as solvent. 1-10 mg/mL concentration used as triplicates through Liquid Phase Epitaxy Drop Casting (LPE-DC) and Solution Evaporation-Liquid Phase Epitaxy (SE-LPE). At lower concentration such as 1mg/mL, 2 mg/mL, 3mg/mL crystallization experiments resulted Form II. At medium dilution 4 to 7 mg/mL resulted dendrites and single crystals of Form I as major and minor as Form II. Above the medium all the time we observed Form I completely. All the experiments where the APAP form I concentration low or medium if it nucleates as Form I ended with dendrites. Form II LPE-DC experiments gave spherical agglomerates and those gave short range in order confirmed by PXRD experiments.

Raman Spectra. The Raman microscope (Kaiser Optical Systems, Inc.) is equipped with a 785 nm exciting line using a 600 grooves/mm grating and a 20X microscope objective. The spectra of the APAP polymorphs Form I, II were collected in a spectral range from 100 to 1200 cm^{-1} , Figure S13 is spectral comparison of the Form I and II. Figure 14 is the needle crystals and block crystal of the Form II which used for Raman spectral analysis.

Powder X-Ray analysis, film X-Ray analysis: Powder X-Ray diffraction (PXRD) patterns were collected with a PANalytical X'Pert PRO Theta/Theta PXRD system with a $\text{Cu K}\alpha$ X-ray source at 45 kV and 40 mA and an X'Celerator high-speed detector. The powder samples were finely ground to spread evenly onto standard zero-background sample holders, and PXRD patterns were obtained for a 2θ range from 5° to 50°. SURMOF samples were collected with no spin single stage flat surface method.

Single crystal analysis:

Single-crystal X-ray diffraction data (Φ and ω scans) of the Form II was collected at 100 K on Bruker Apex-II CCD detector diffractometer coupled using Mo K α radiation ($\lambda = 0.71073 \text{ \AA}$) from. Face indexing has been done by Apex-III, data reduction and crystal structure was solved and refined direct methods using SHELXTL 2014.¹ A check of the final crystallographic

information file (CIF) with PLATON (Spek, 2009) did not show any missed symmetry. Mercury was used to prepare the figures and packing diagrams. Crystallographic parameters of the Form II summarized in Table S4. CIF file deposited, CCDC No. 1814819.

AFM analysis and SEM analysis: Atomic Force Microscopy (AFM) Analysis of substrate SURMOF films were analyzed with AFM to know surface uniformity and distribution of MOF. AFM images were obtained with a Dimension 3100 XY closed-loop scanner (Nanoscope IV, Veeco) equipped with Nanoscope software (Veeco Instruments, Inc.). Height and phase images were obtained in tapping mode in ambient air with silicon tips (Veeco), and roughness and phase changes were analyzed using Nanoscope software. SEM images of the substrate surfaces and APAP crystals, dendrites, Form II agglomerates, spherical particles were collected at different magnifications. SEM samples were done JEOL 6060 SEM at a 5 kV operating voltage for surface image EDX elemental analysis.

QCM Quartz Crystal Micro balance: QCM crystal was washed the same way of SAM cleaning procedure and further went ahead for all the experiments. The synthesis of the HKUST-1-1 SURMOF was interrupted after 6 cycles and Metal(A)-wash-Ligand(B)-wash-APAP(C) as A-B-C-A-B-C- etc., each step 8-10 min interval nearly. 10 mmol solution of $\text{Cu}(\text{OAc})_2$, H_3BTC , APAP in EtOH was prepared and experiments were performed at 22 °C and the flow rate was maintained constant at 200 mL/min deposition on Au coated electrodes. The inset shows the corresponding Eyring–Polanyi plots for each of the individual deposition steps. Same procedure was followed for unmodified and modified first two experiments as well.

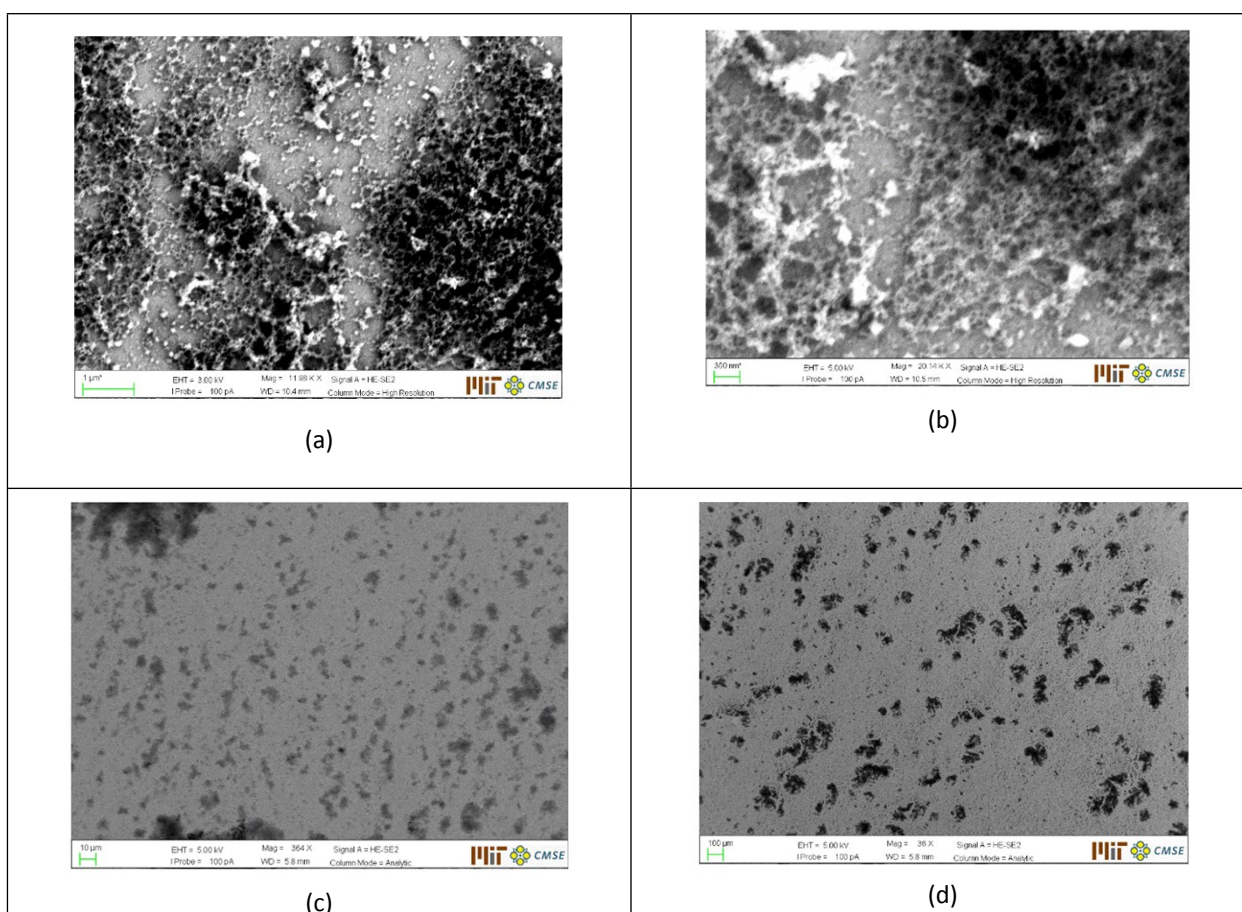
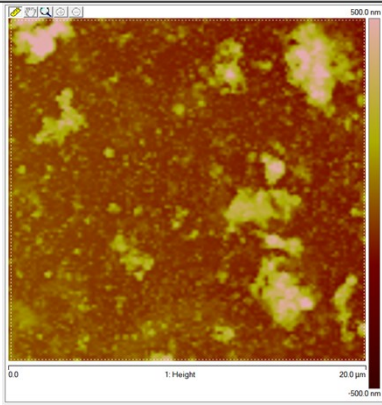
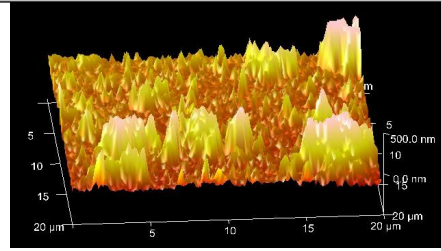


Figure S1. SURMOF thin film surface was monitored by SEM examined by different films in different magnification to conform the particle size, smooth and the height and particles in nm scale after 20 layers. (a), (b) Displayed in nanometer scale of MOF and growth of film confirms the porous coordination polymer at different places of duplicates. Nano porous surface exhibited 700-800 nm height and thus we have used 10 layers template surfaces for all the study. (c), (d) Film at lower magnification in duplicate samples.

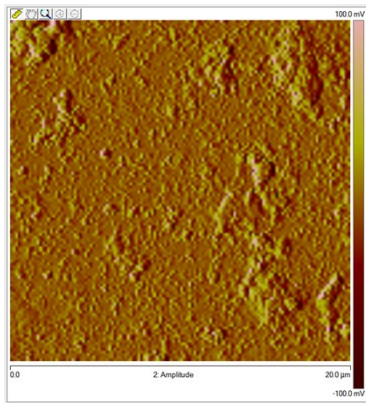
Film I	



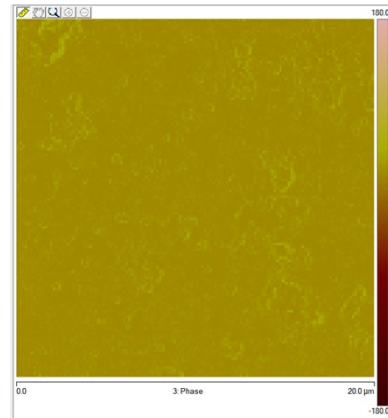
Surface image



3D image to know height

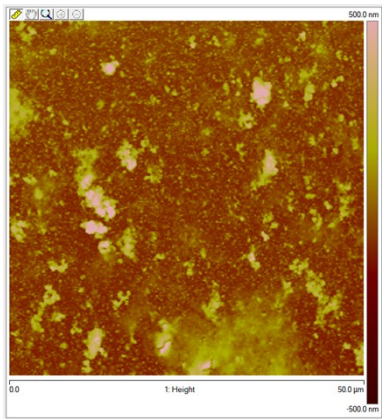


Amplitude

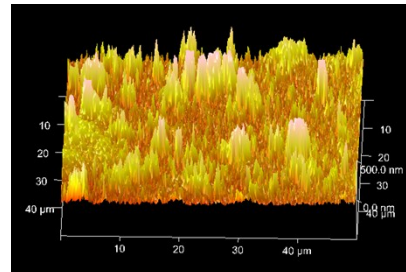


Phase purity

Film II



Surface image



3D image to know height image

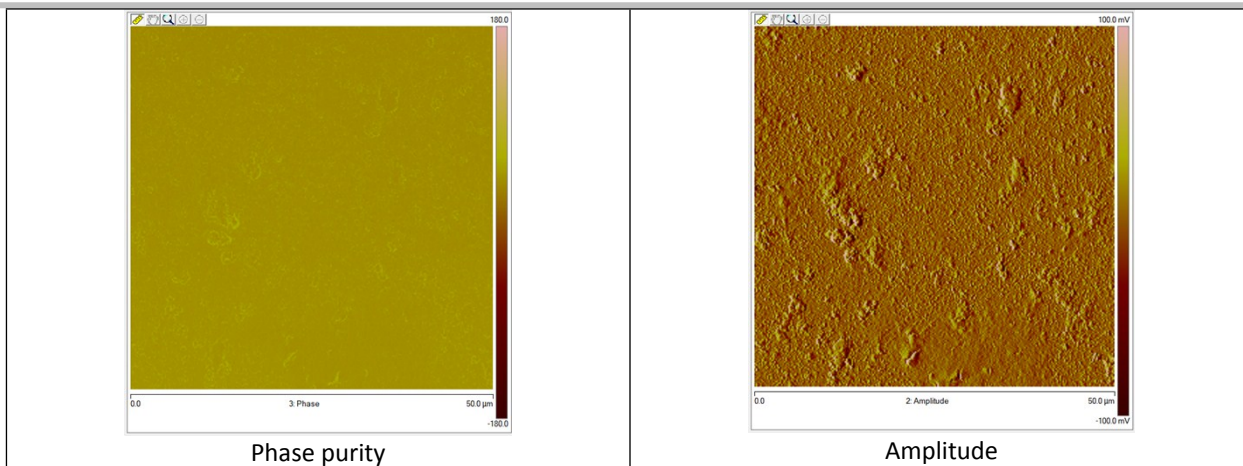
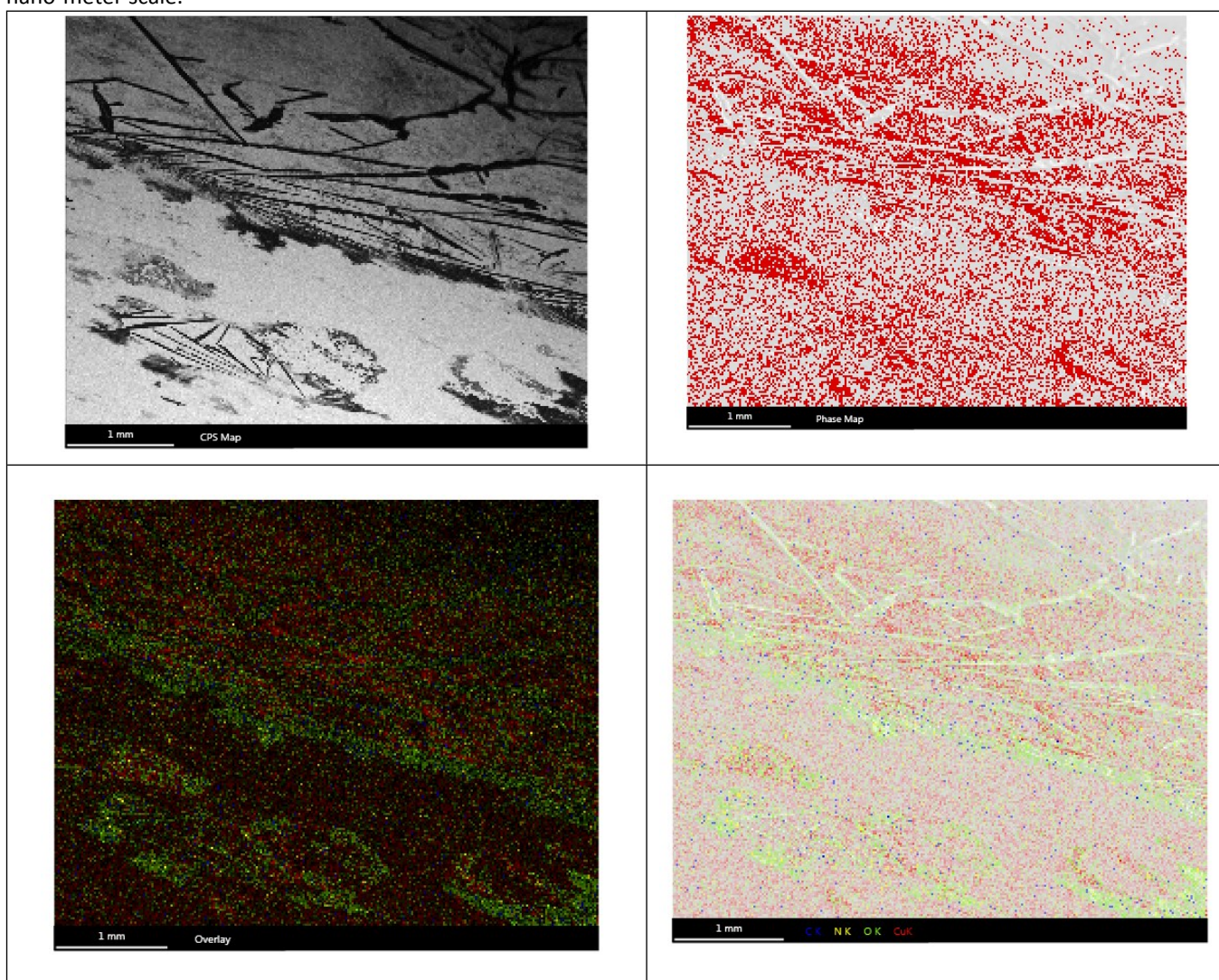


Figure S2. AFM analysis of the two different SURMOFs are performed and confirm the phase purity and height of the film in nano-meter scale.



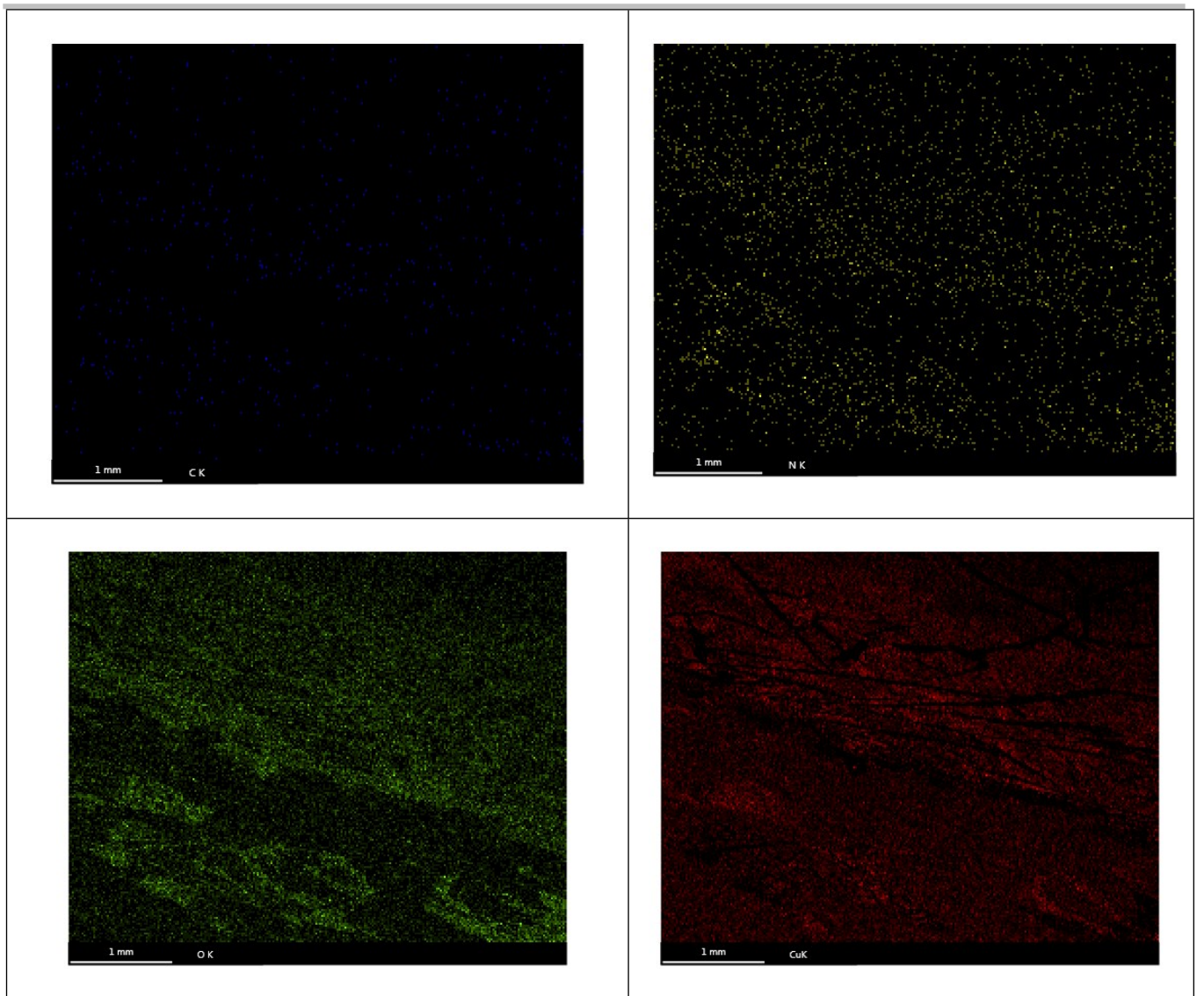
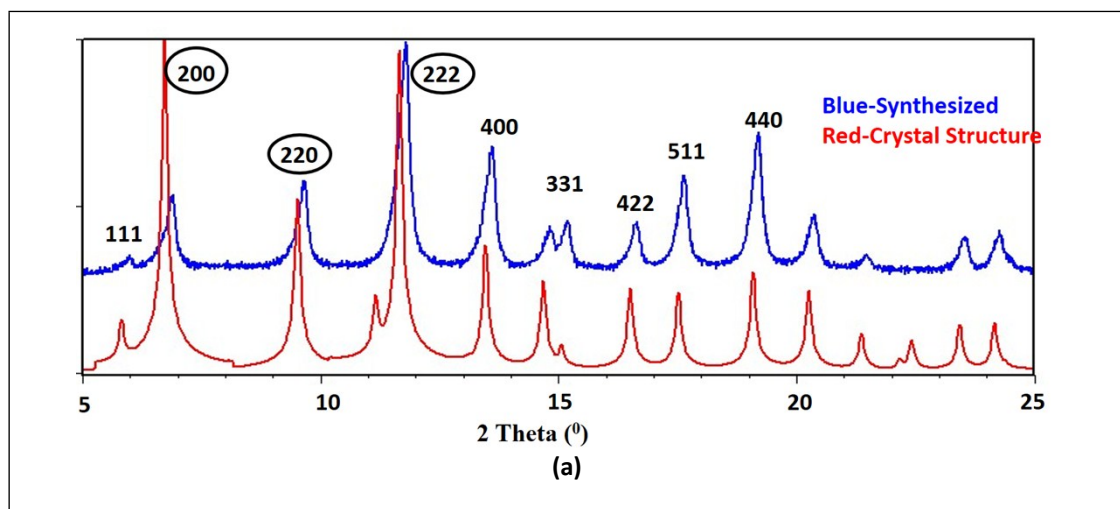


Figure S3. SEM EDAX analysis of the SURMOF films to confirm the uniform distribution of the MOF. Elemental analysis confirms the distribution of the CU, C, O, N atoms.



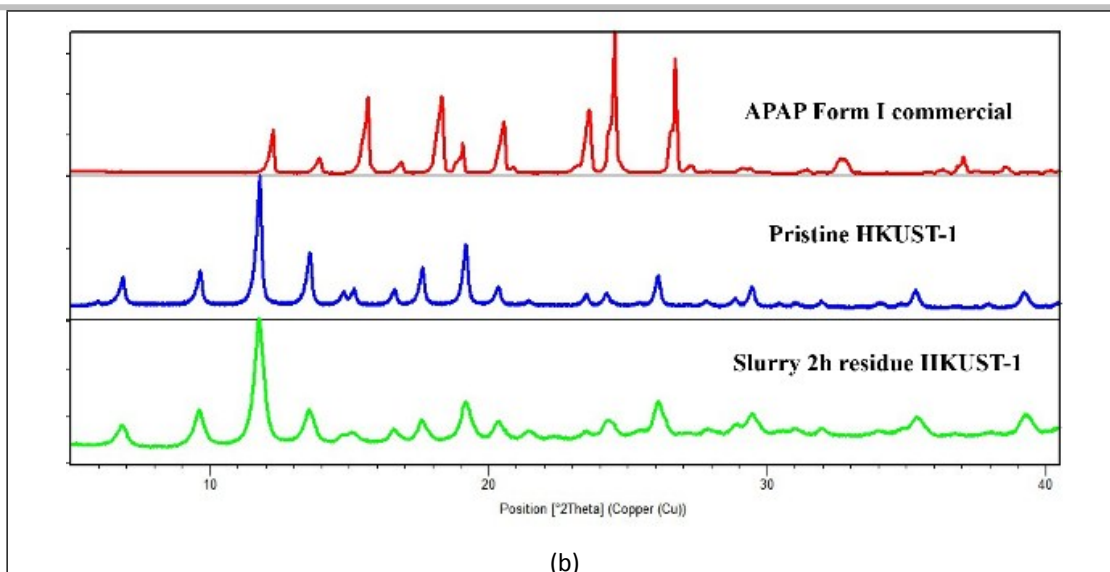
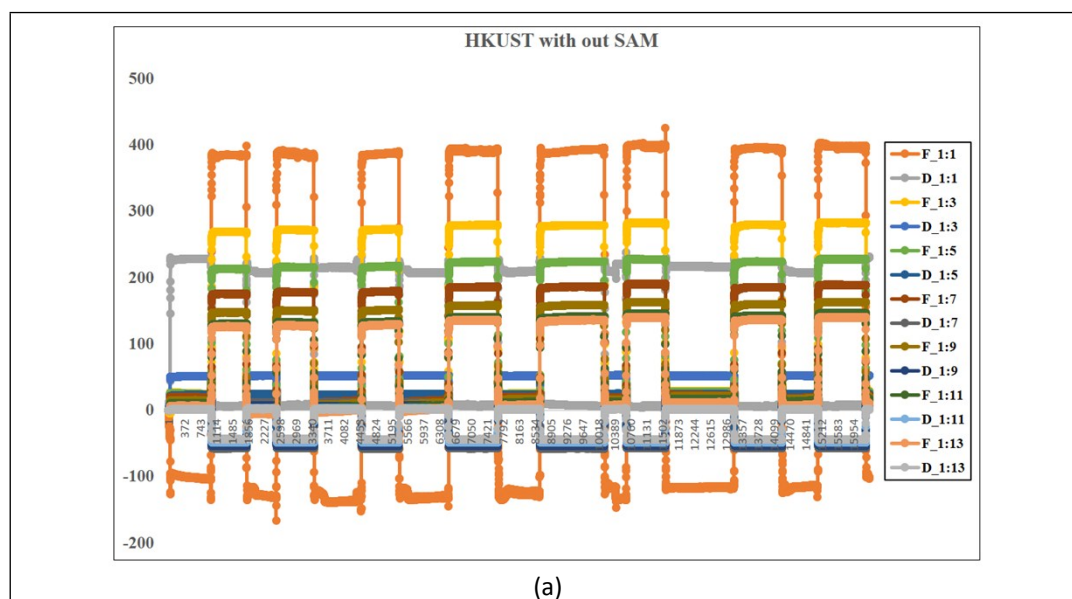


Figure S4. (a) XRD comparison of the Pristine HKUST-1 and reported pattern. Matching of the both 2θ values confirms the purity of the prepared MOF in present study. (b) XRD comparison of the APAP and Pristine HKUST-1 with slurry of 50:50 mg APAP: HKUST-1 slurry residue 6h in EtOH. Which confirms the pure HKUST-1 and there was no complexation with APAP.



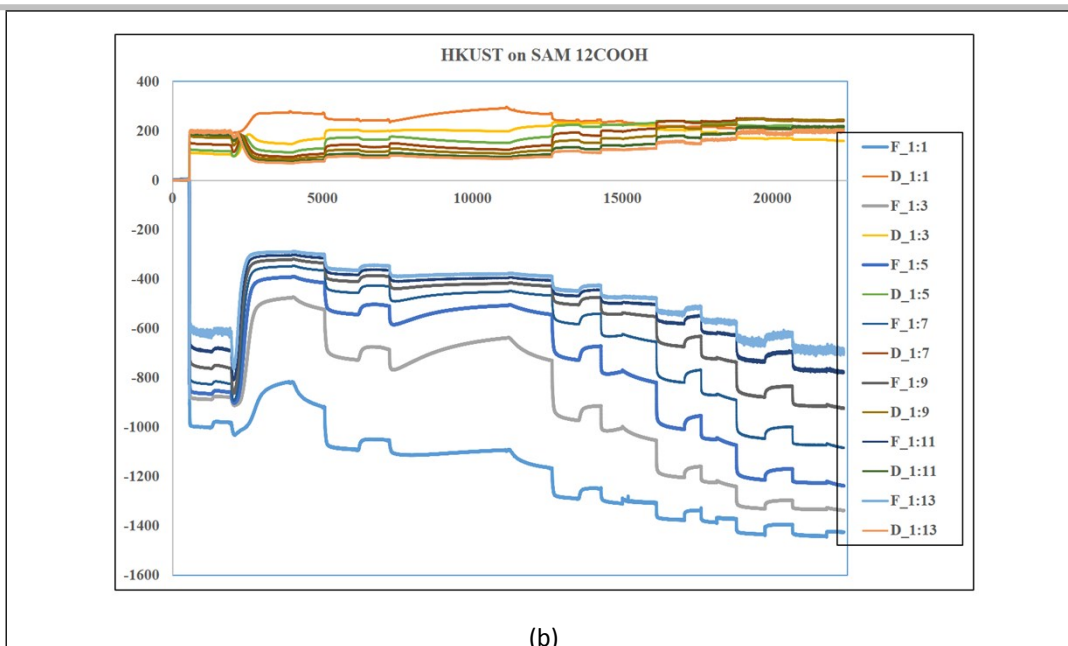


Figure S5. QCM-D experiments of the HKUST-1 MOF with bare gold, without SAM layer suggests deposition of the metal layer was removed during wash cycle and same trend with ligand also. This experiment supports advantage of the SAM for topo chemical reactions. (b) MOF deposition with SAM surface and confirms the continuous addition of metal and ligand solutions gave decrease in frequency confirm layer MOF preparation. F=Frequency and D=Dissipation. Various F, D was measured.

Table S1. Results observed present study and reported literature.

Name	Form	Crystallization from solution observed present study	Crystallization with SURMOF observed present study	Usual morphology reported	Observed in present study with SURMOF
Acetaminophen	I	Predominantly from most of the solvents	Observed at high super saturation	Blocks, plates, rods depends on high, medium, low super saturation	Dendrites at medium and Blocks at high super saturation
	II	Rare case with Ethanol solvent and concomitant with Form I	Predominantly observed from EtOH at low super saturation	Needles	Blocks, plates

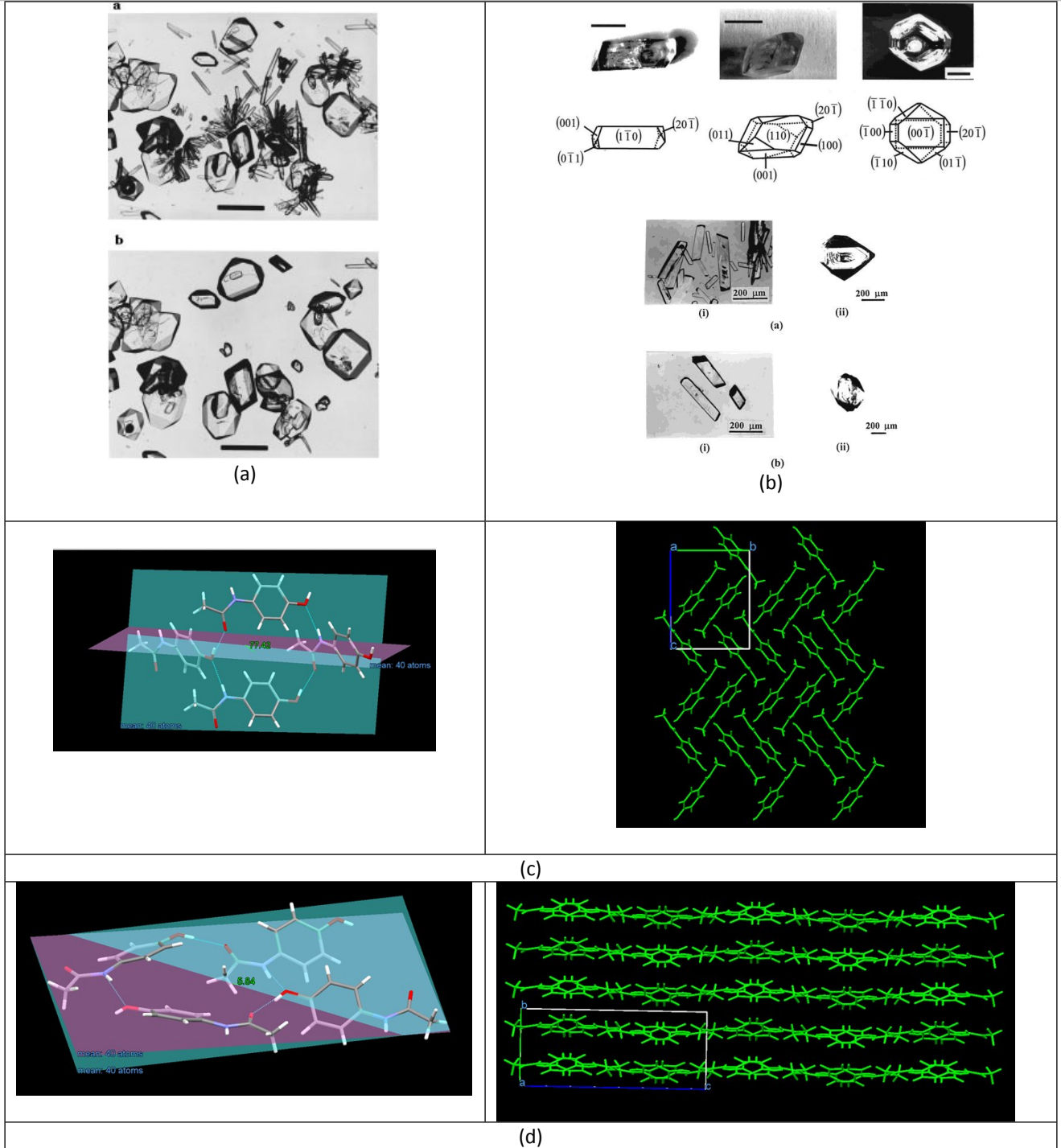
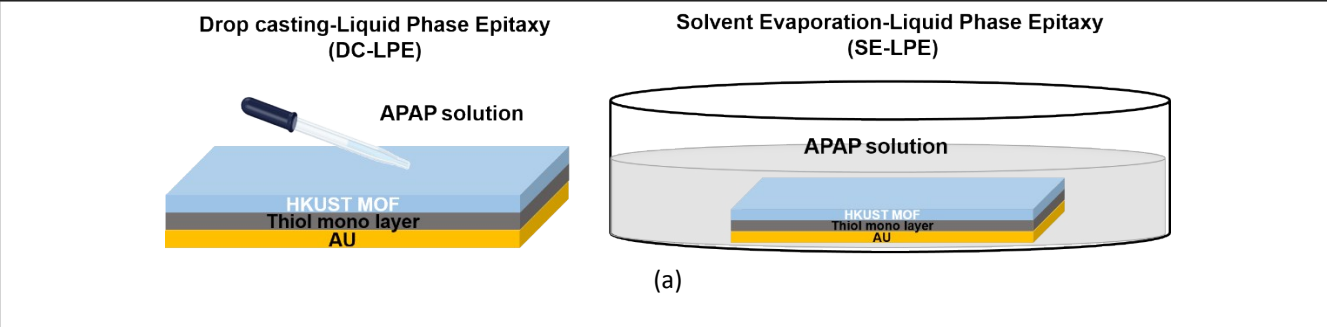


Figure S6. (a)^[2], (b)^[3] Reported morphologies of Form I, II (c) packing analysis of the FORM I. (d) Packing analysis of the Form II.



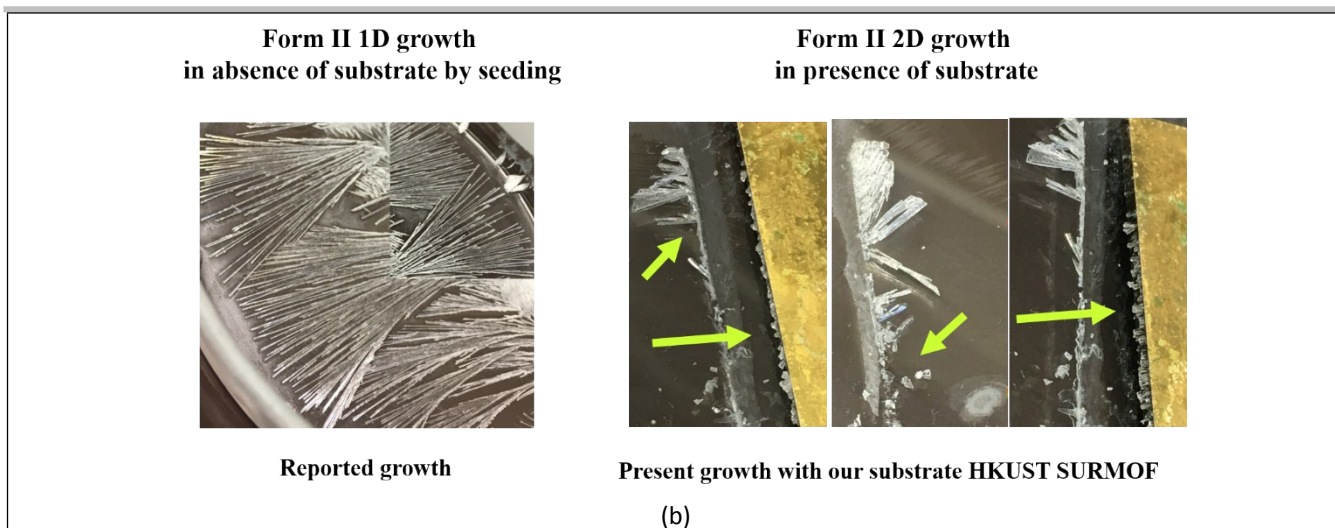
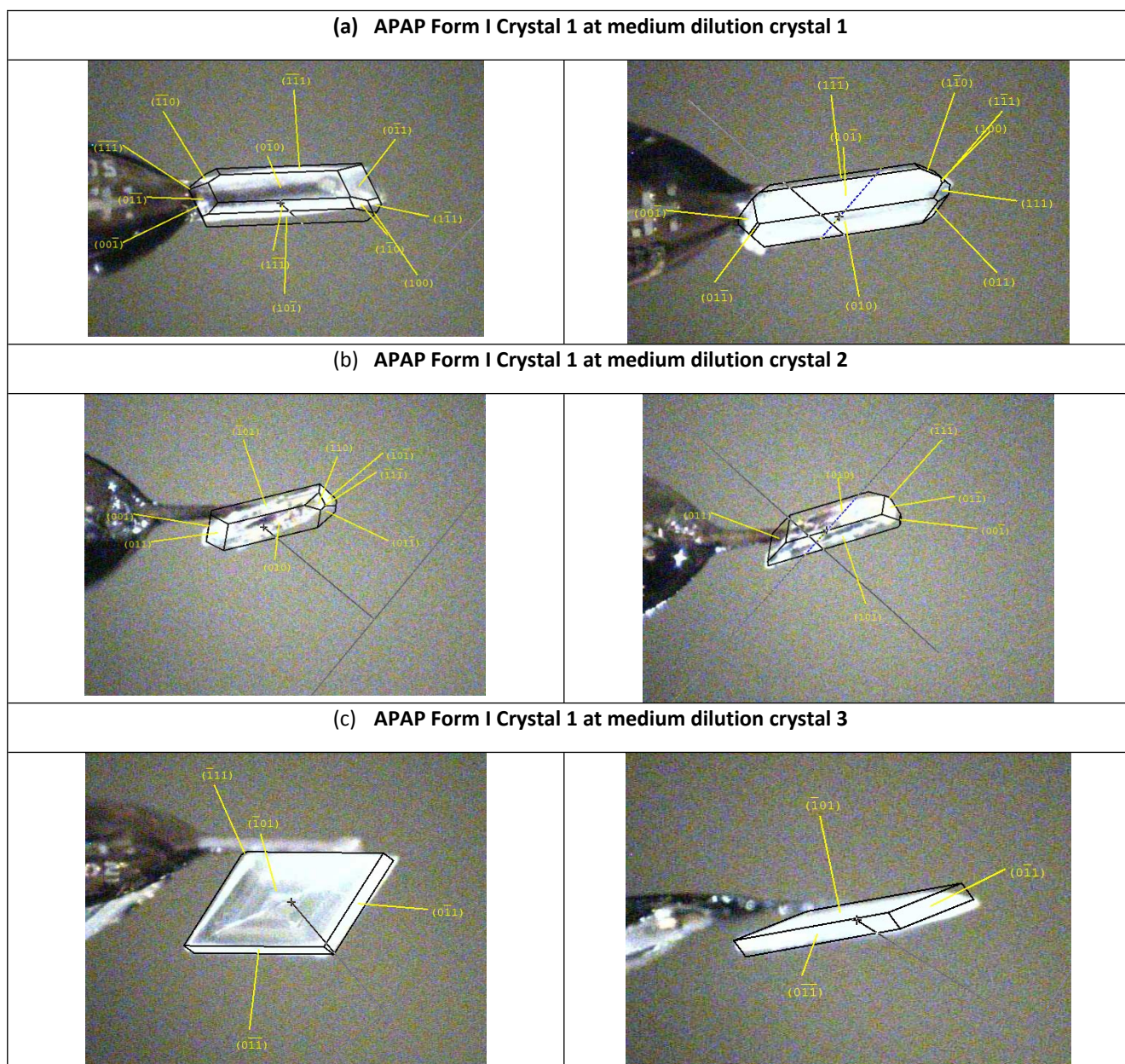
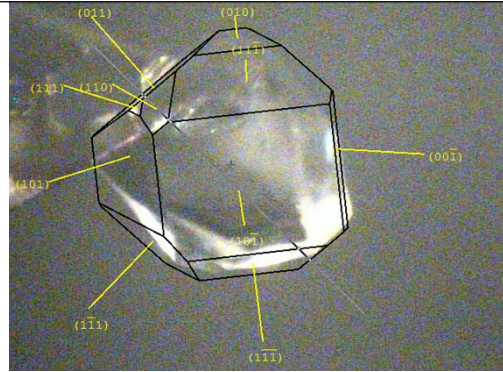
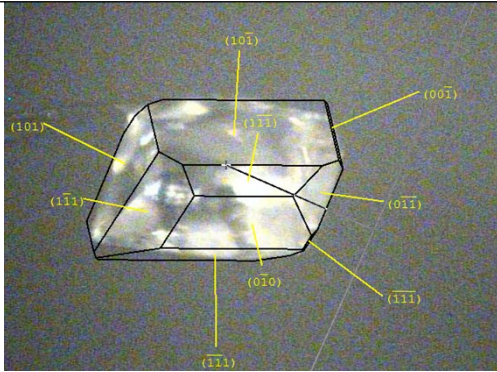


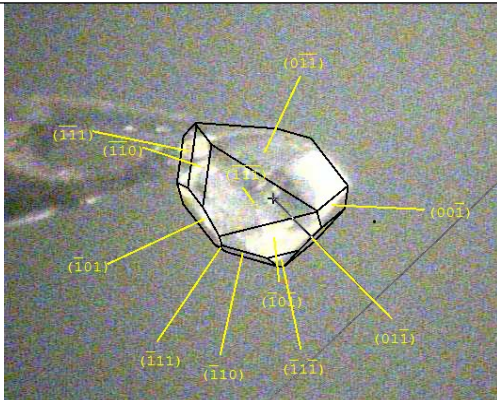
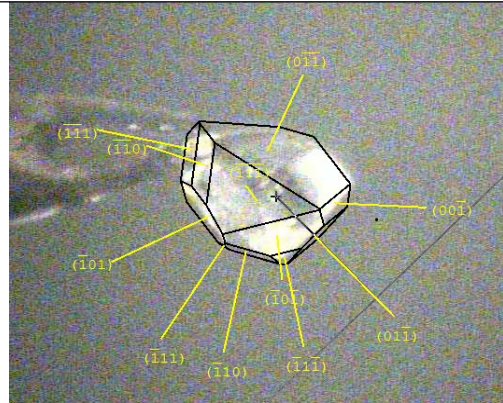
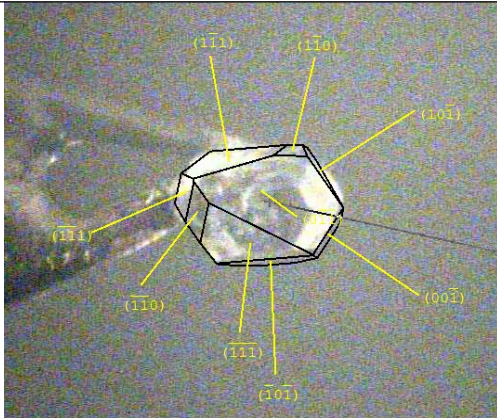
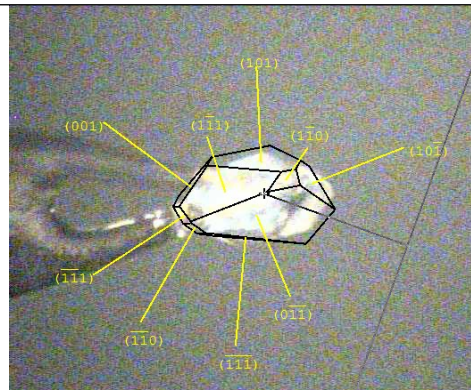
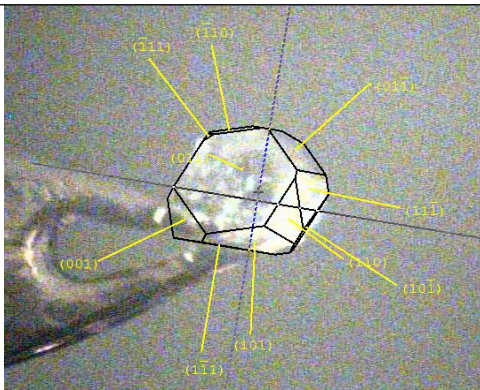
Figure S7. (a) Crystallization methods used to prepare Form I, II. (b) Form II synthesized by seeding, crystal grown at the edge of the SURMOF was seeded. This experiment confirms without designed substrate 1D needles are common. (b) crystals grown at the edge of the substrate as block crystals.



(h) APAP Form I Crystal 1 at medium dilution crystal 8 at edge



(i) APAP Form I Crystal 1 at medium dilution crystal 9 at rest of the place of bottem where no influence of SURMOF



(j) APAP Form I Crystal 1 at medium dilution crystal 10 at edge

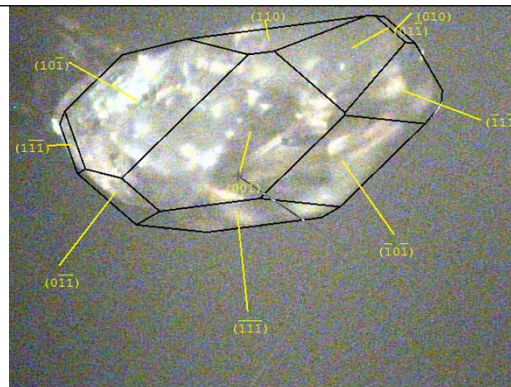
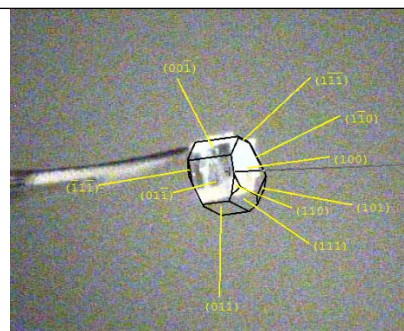
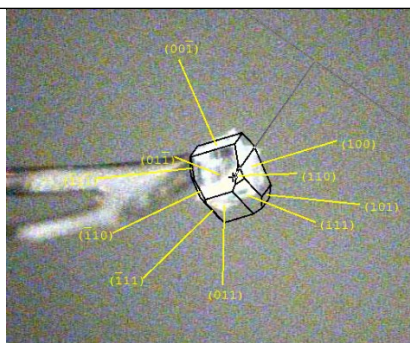
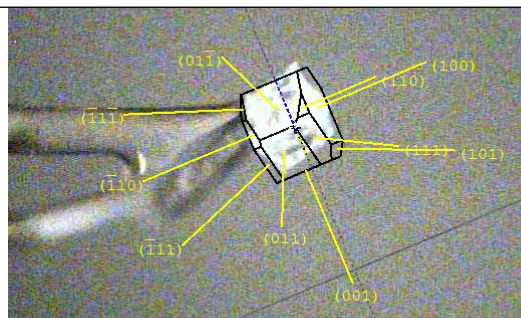
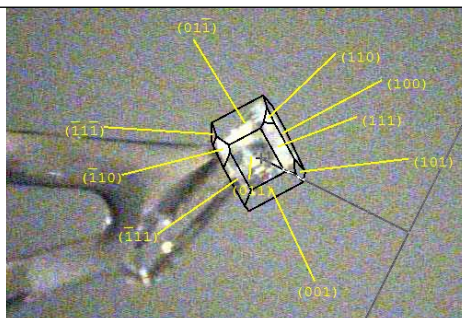
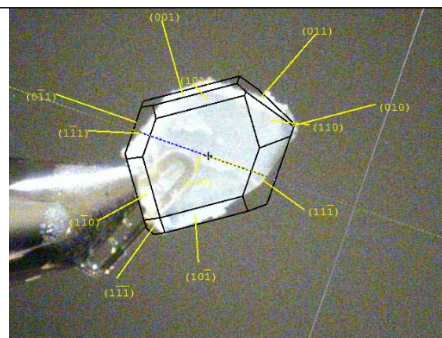
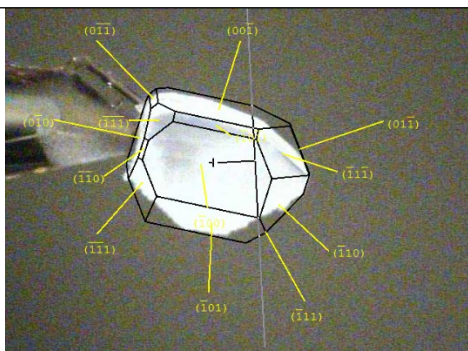


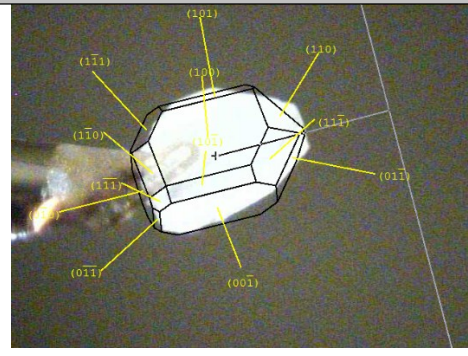
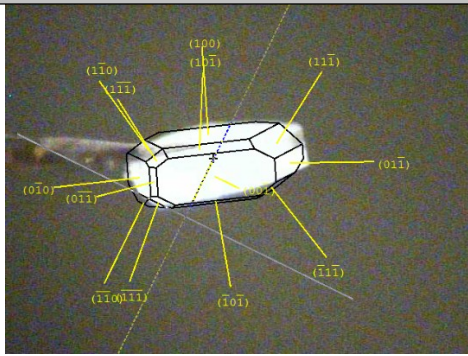
Figure S8. Face indexed single crystals of the Form I.

(a) APAP Form II Crystal 1

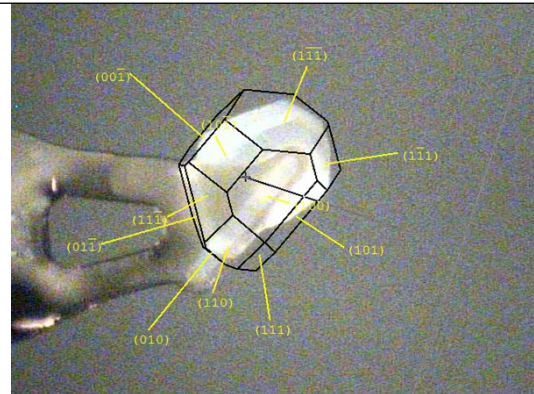
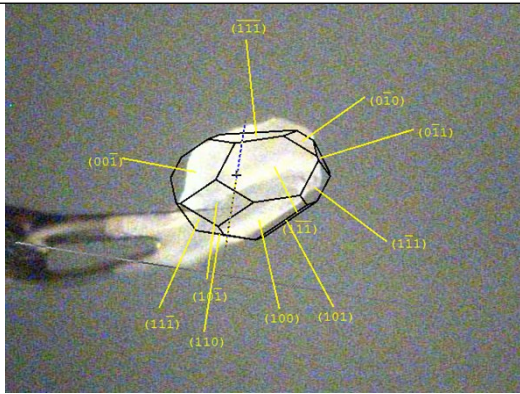
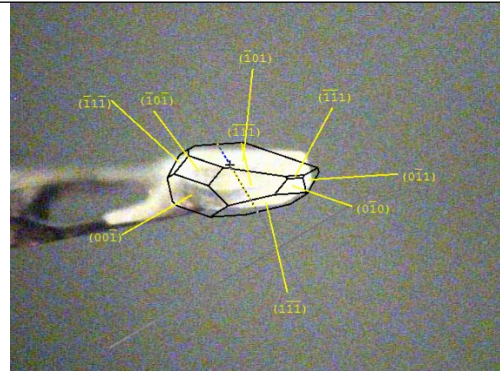
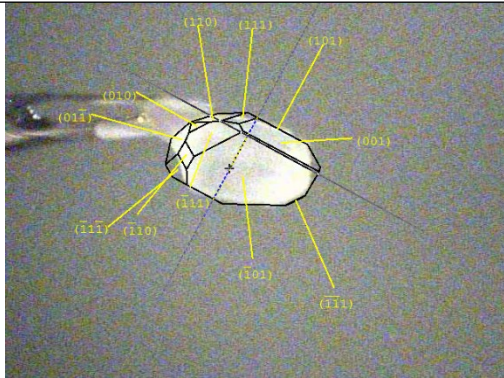


(b) APAP Form II Crystal 2

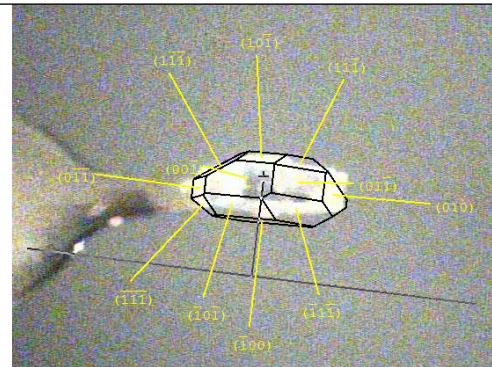
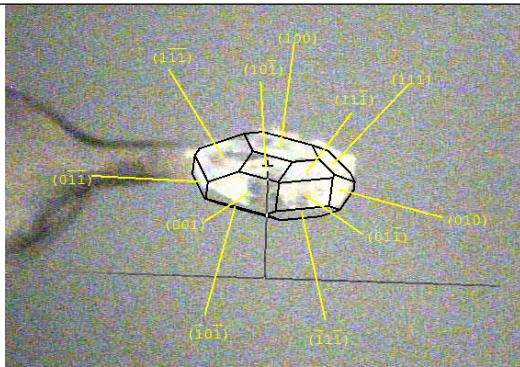


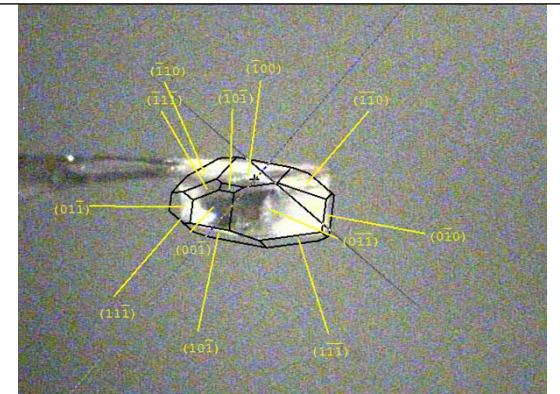
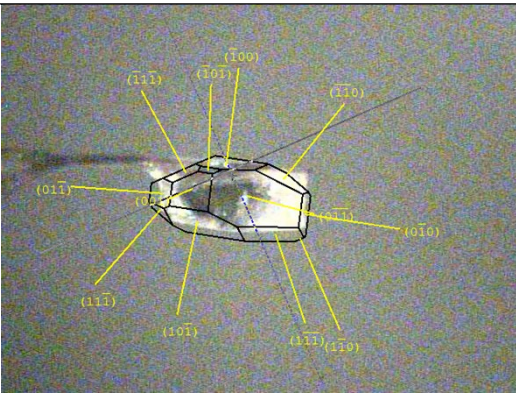
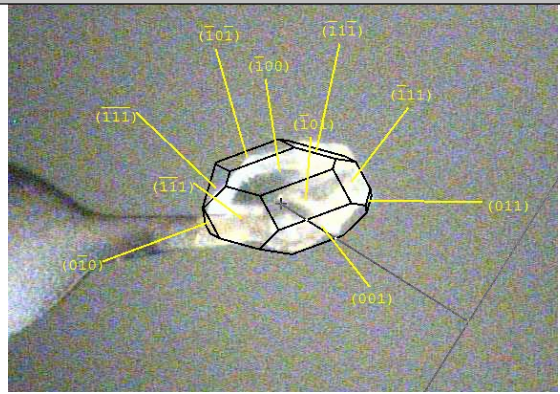
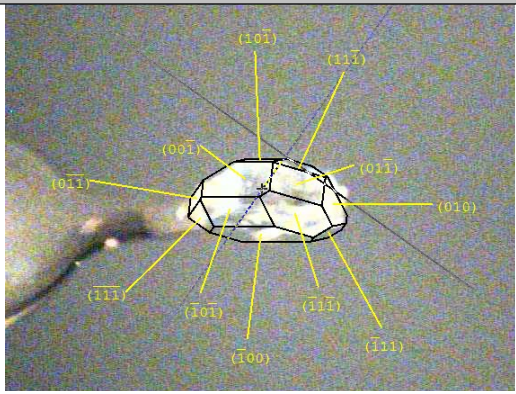


(c) APAP Form II Crystal 3

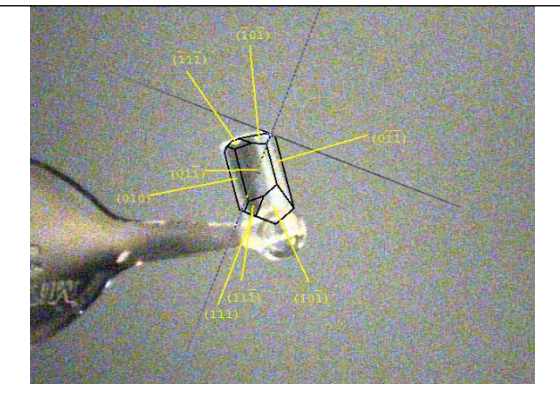
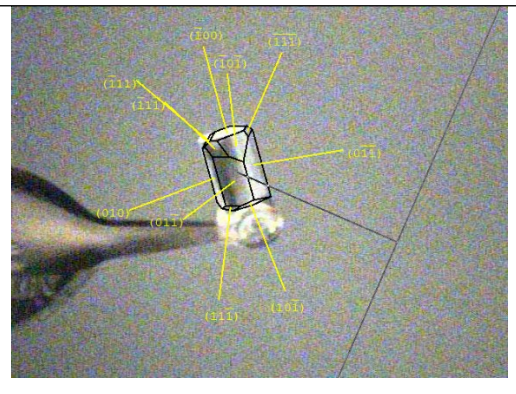


(d) APAP Form II Crystal 4

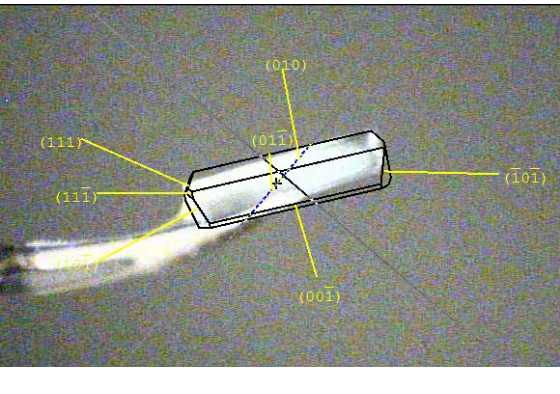
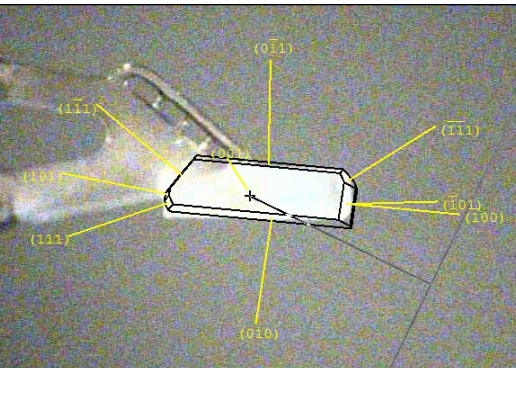


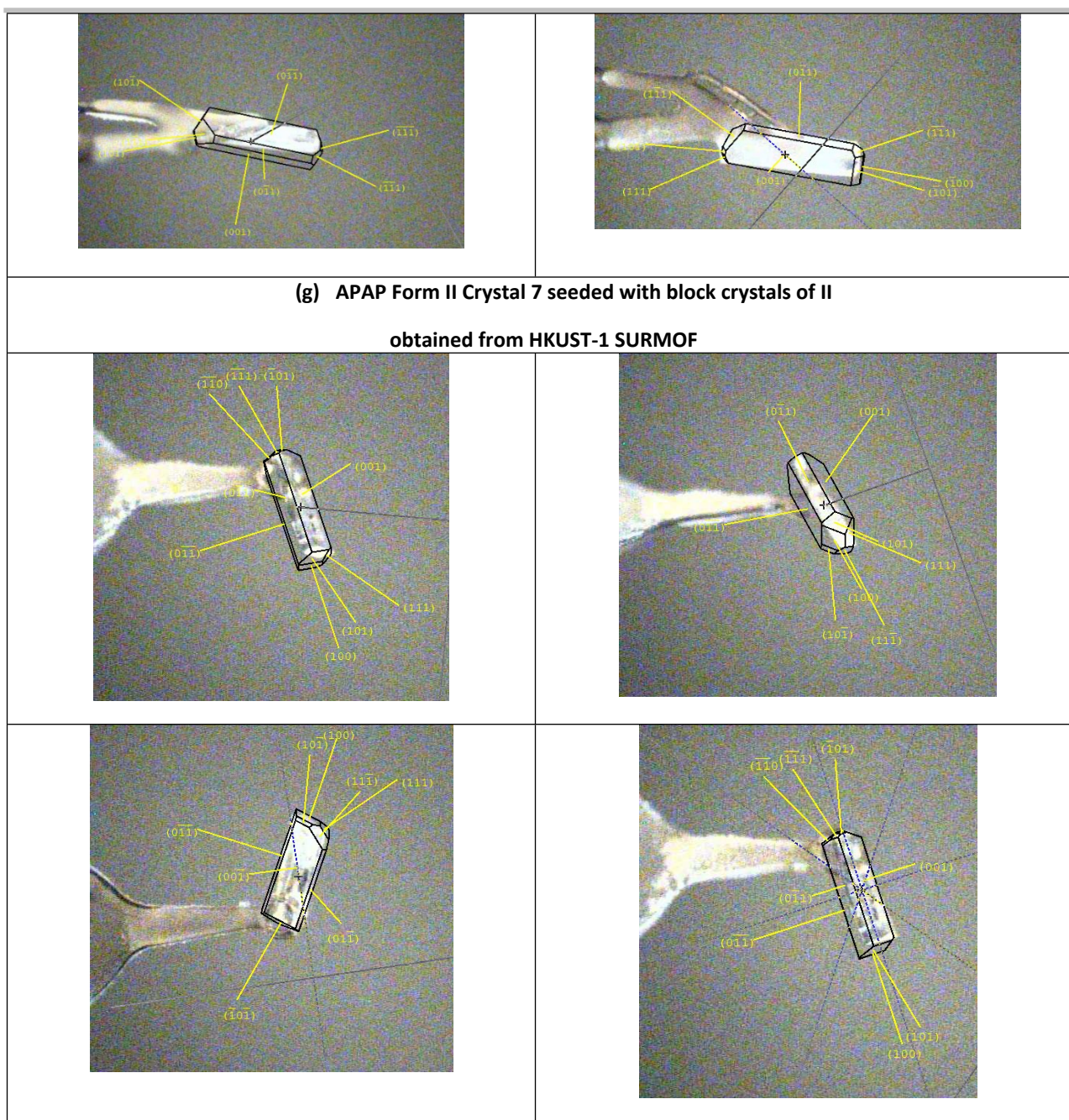


(e) APAP Form II Crystal 5



(f) APAP Form II Crystal 6





(g) APAP Form II Crystal 7 seeded with block crystals of II
obtained from HKUST-1 SURMOF

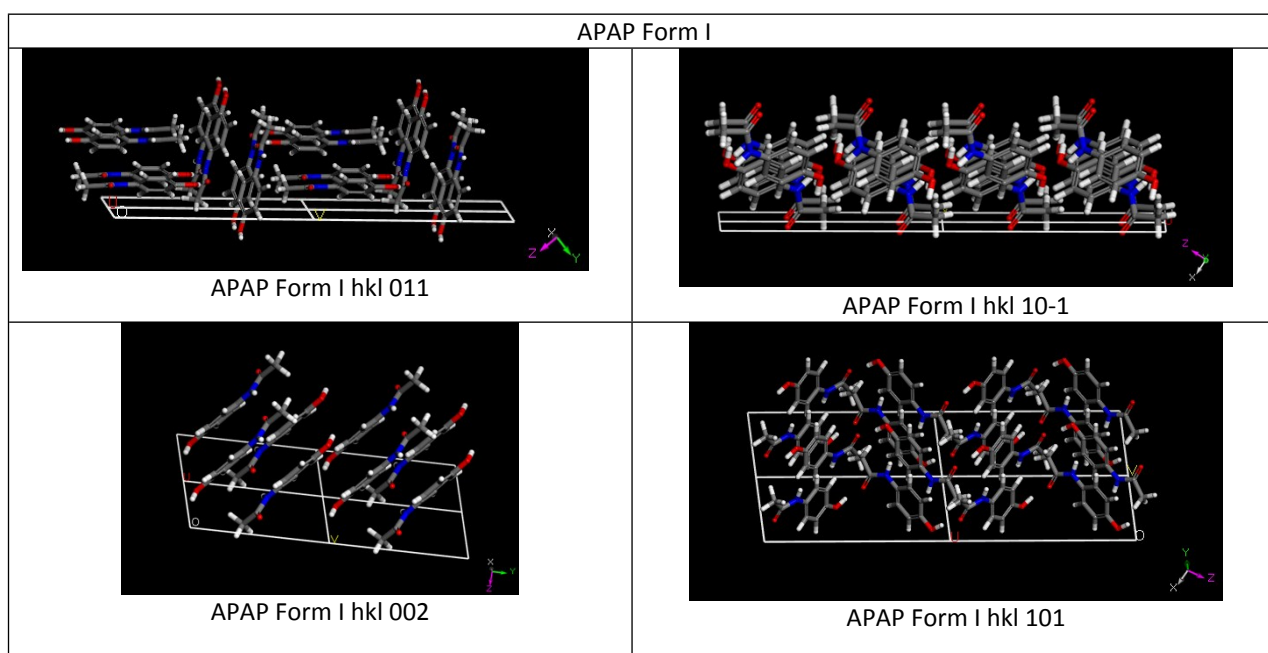
Figure S9. Face indexed single crystals of the Form II.

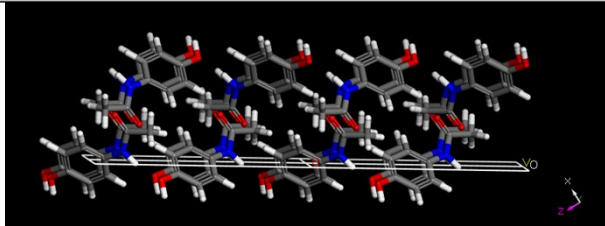
Table S2. Summary of the faces resulted in presence and absence of SURMOF substrate.

	Without SURMOF HKUST-1		With SURMOF HKUST-1		Calculated from Material studio, Morphology growth basis on attachment energy	
	Major faces	Minor faces	Major faces	Minor faces	Major faces	Minor faces
Form I	010, 1-1-1, 101, -1-11,	011, 100, 001, 1-11, -1-1-1	111, 011, 110, 10-1, 101	100	011, 101, 020	002, 012, 111
Form II	0-11, 010, 001	100, 101, 111	100, 101, 001	011, 111, 110	002, 102, 200, 111, 112, 020	210, 112, 202, 211, 113, 212

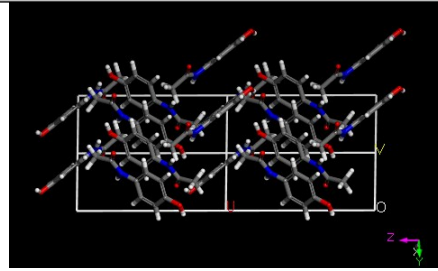
Table S3. Attachment energy calculations of the Form I, II performed on Material Studio.

	Hkl	Eatt (Total) Kcal mol ⁻¹	Total facet area	% Total facet area
Form I	{011}	-52.142	2.600822e+004	44.81978464
	{10-1}	-67.612	7.610241e+003	13.11467545
	{002}	-80.566	329.45549678	0.56774837
	{101}	-53.107	1.241876e+004	21.40116651
	{110}	-69.325	4.518530e+003	7.78675073
	{11-1}	-73.612	1.378291e+003	2.37519922
	{012}	-71.586		
	{111}	-72.248		
	{020}	-54.437	5.764937e+003	9.93467508
	{021}	-66.040		
Form II	{002}	-148.355	3.907830e+004	14.65268909
	{102}	-157.486	2.028067e+004	7.60438368
	{200}	-104.065	6.623418e+004	24.83497972
	{111}	-126.878	1.144887e+005	42.92835981
	{112}	-163.194		
	{202}	-177.785		
	{210}	-139.206	73.99387163	0.02774453
	{211}	-159.885		
	{113}	-181.466		
	{212}	-176.266		
	{020}	-116.607	2.654128e+004	9.95184318

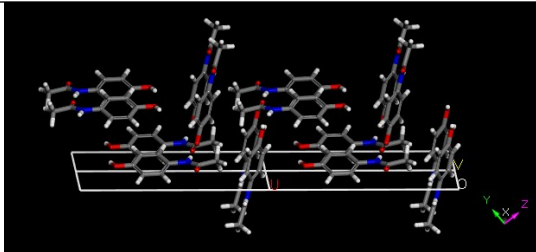




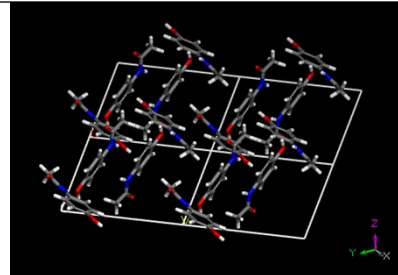
APAP Form I hkl -101



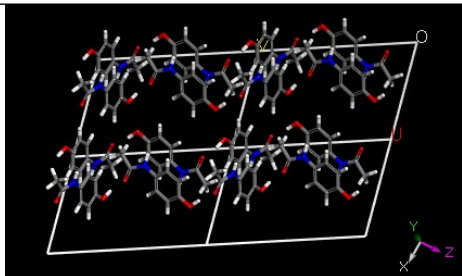
APAP Form I hkl 110



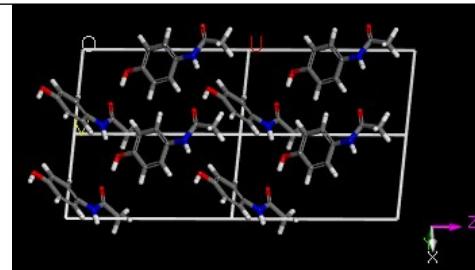
APAP Form I hkl 0-1-1



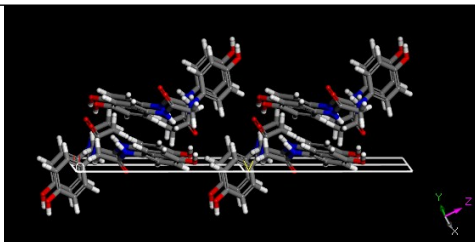
APAP Form I hkl 11-1



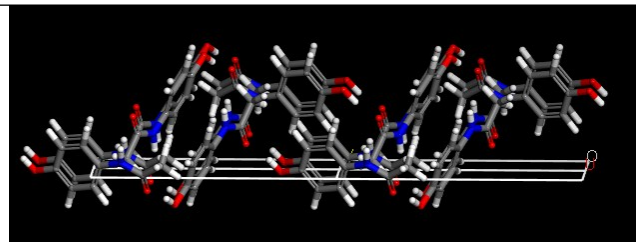
APAP Form I hkl 111



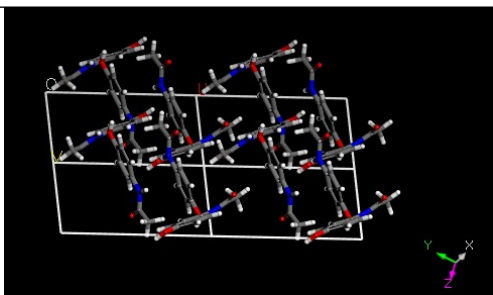
APAP Form I hkl 020



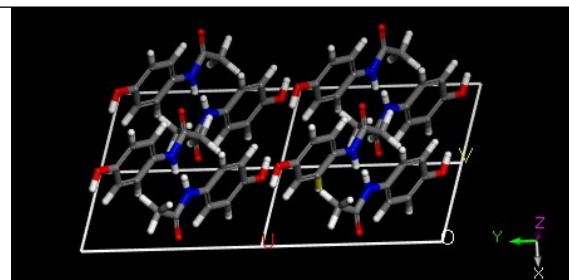
APAP Form I hkl 1-1-1



APAP Form I hkl -11-1

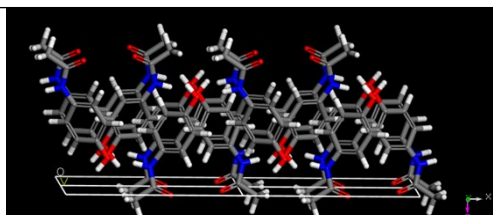


APAP Form I hkl -1-11

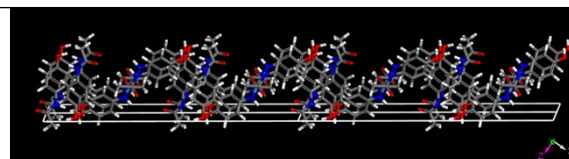


APAP Form I hkl 100

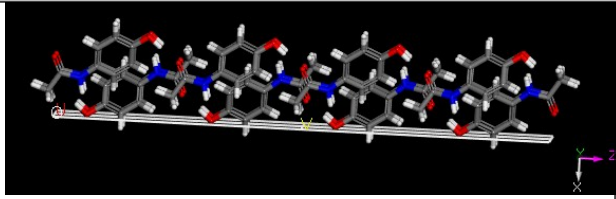
APAP Form II



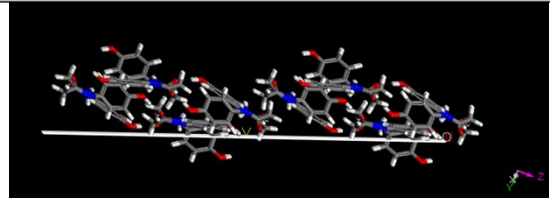
APAP Form II hkl 001



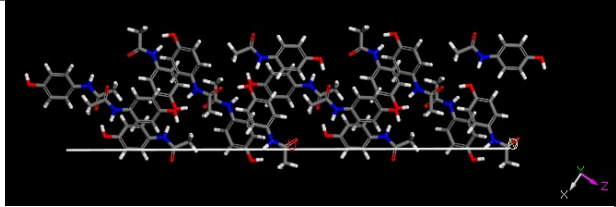
APAP Form II hkl 102



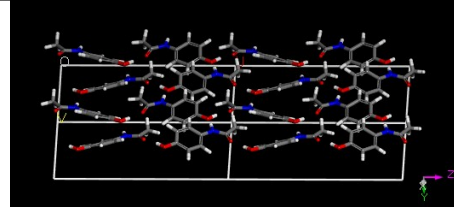
APAP Form II hkl 100



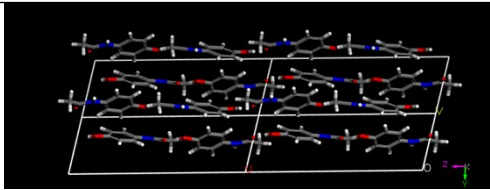
APAP Form II hkl 111



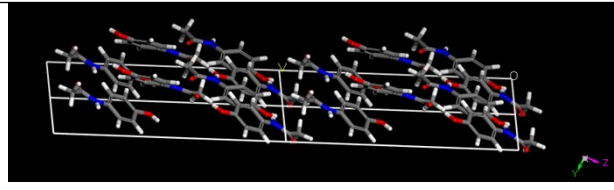
APAP Form II hkl 101



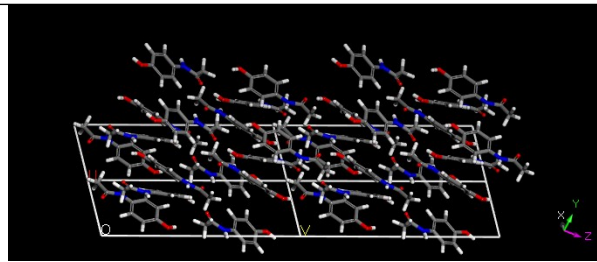
APAP Form II hkl 010



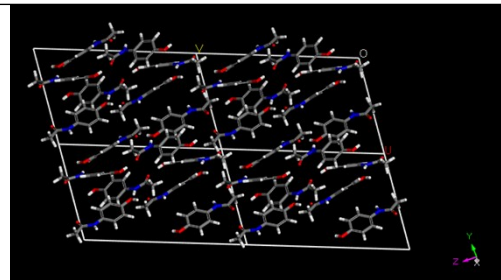
APAP Form II hkl 110



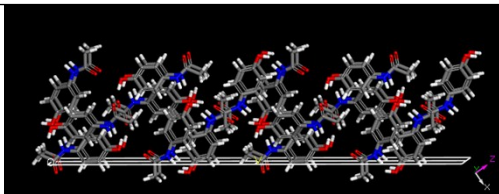
APAP Form II hkl 011



APAP Form II hkl 0-11

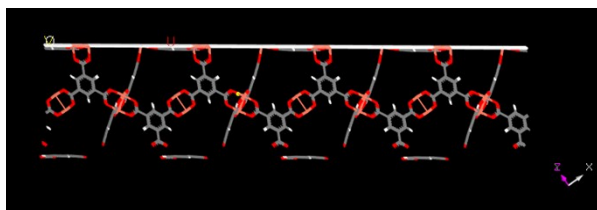


APAP Form II hkl -1-11

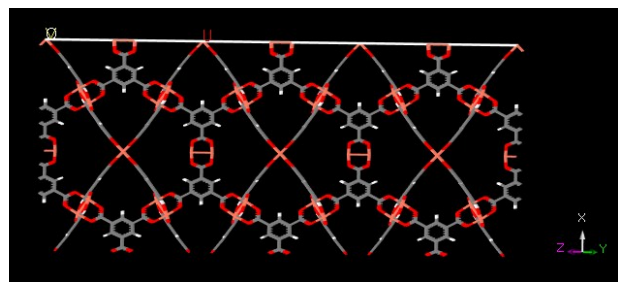


10-1

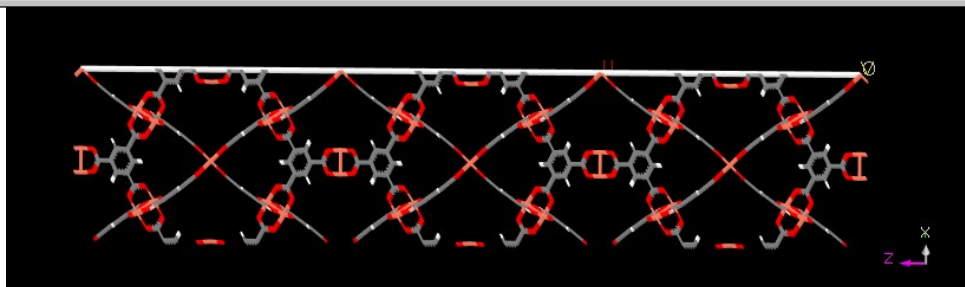
HKUST-1 MOF



HKUST-1 MOF hkl 111



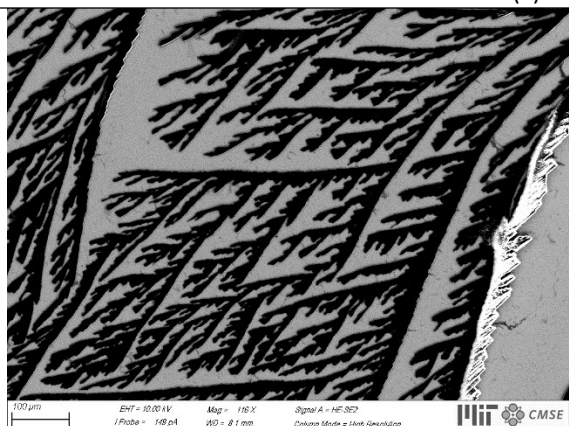
HKUST-1 MOF hkl 100



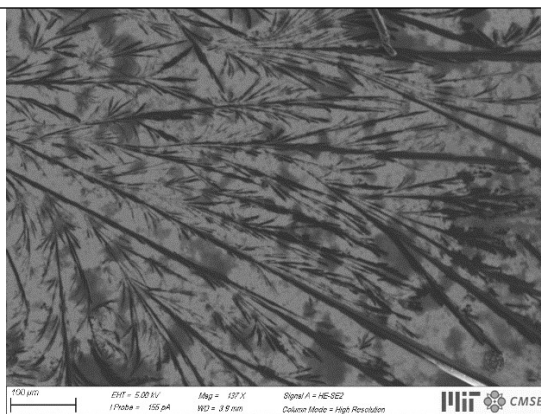
HKUST-1 MOF hkl 110

Figure S10: Material Studio calculations: Attachment energies were calculated by using Material studio after optimization Geometry and morphology growth was performed to know the habit, faces of APAP polymorphs. View of the APAP polymorphs, HKUST-1 MOF faces with hkl values exposed at face boundaries.

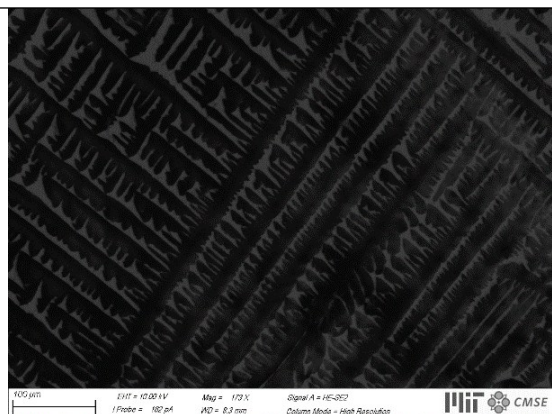
(a) APAP Form I



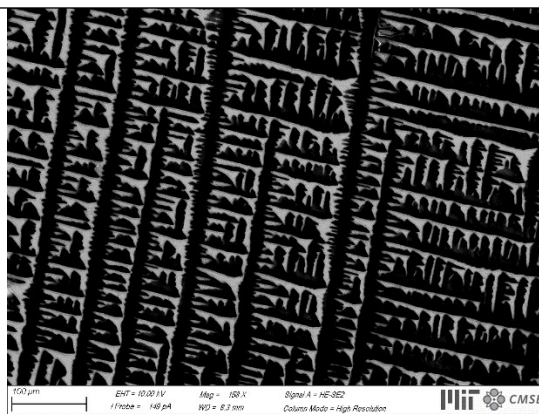
1-Form I dendrites of 10-1 face



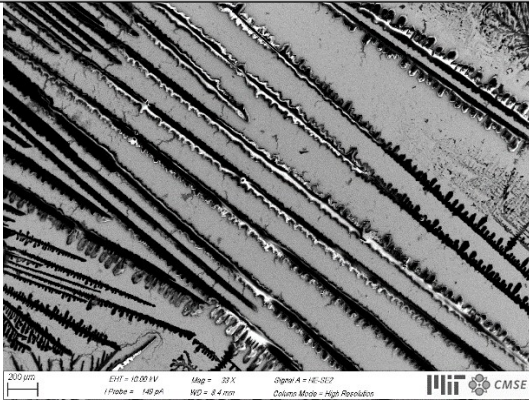
2-Form I dendrites of 10-1 face



3-Form I dendrites of 10-1 face



4-Form I dendrites of 10-1 face



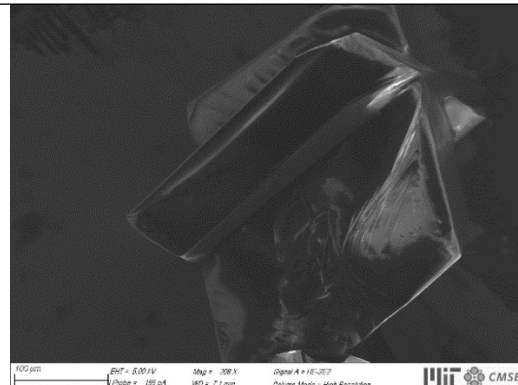
5-Form I dendrites of 10-1 face



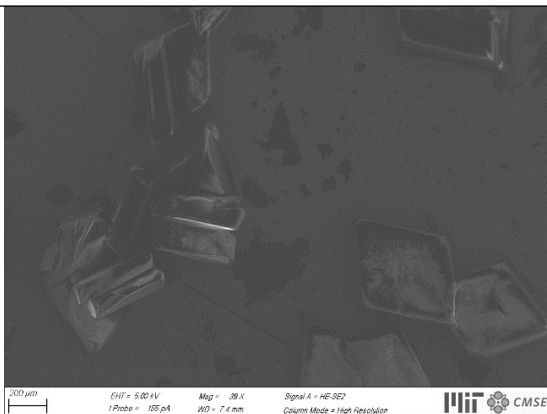
6-Form I dendrites of 10-1 face and rod morphology crystals



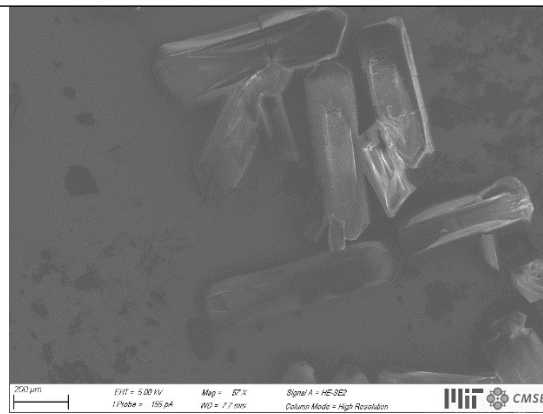
7-Form I dendrites of 10-1 face



8-Form I dendrites of 10-1 face and block, rod morphology crystals

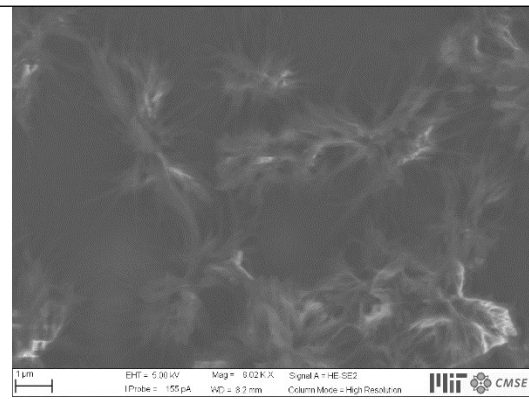
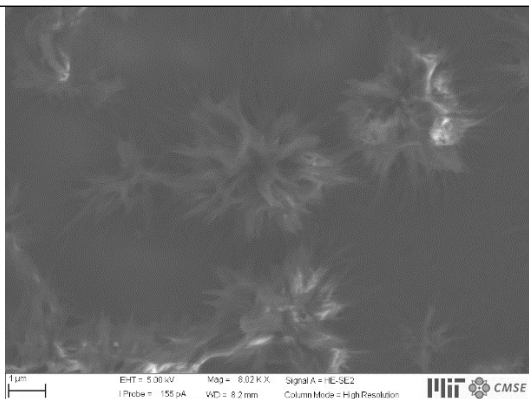


9-Form I block, rod morphology crystals

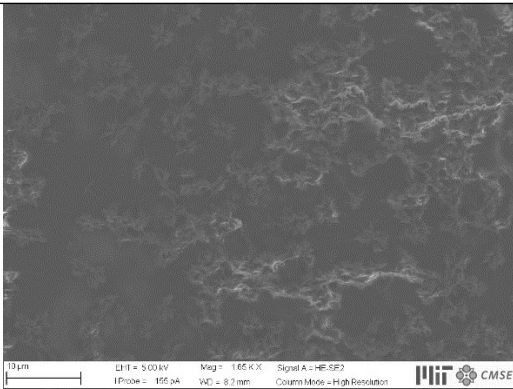


10-Form I block, rod morphology crystals

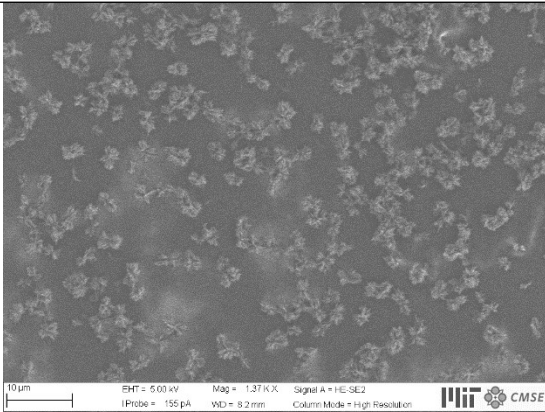
(b) APAP Form II



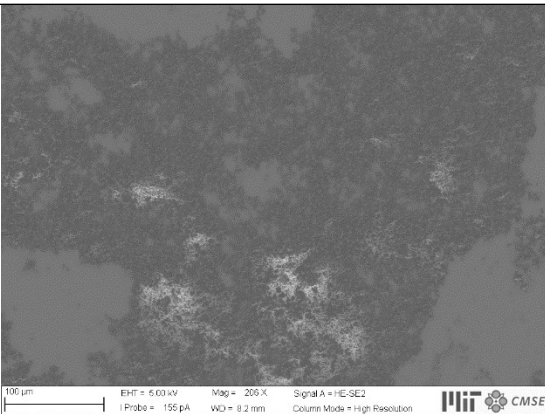
1-Form II spherical agglomerates



3-Form II spherical agglomerates

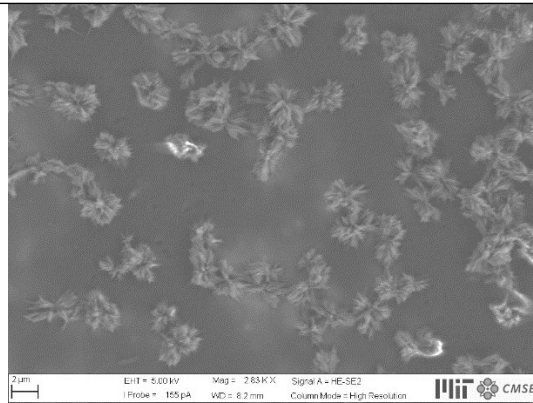


5-Form II spherical agglomerates

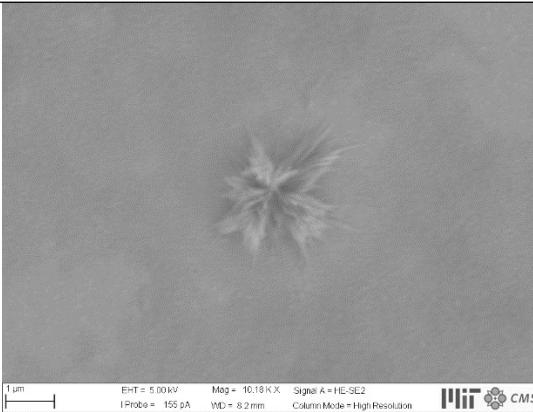


7-Form II spherical agglomerates

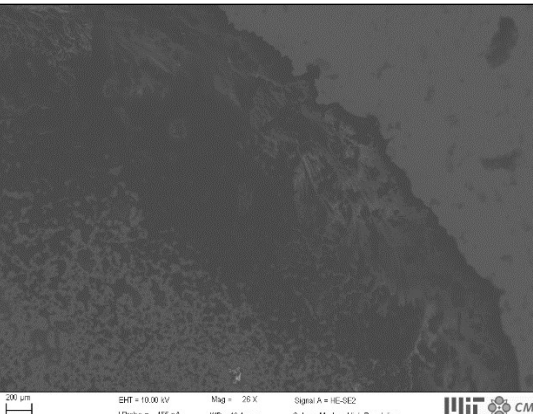
2-Form II spherical agglomerates



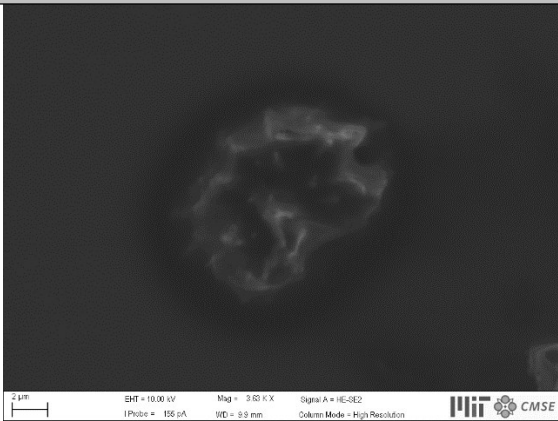
4-Form II spherical agglomerates



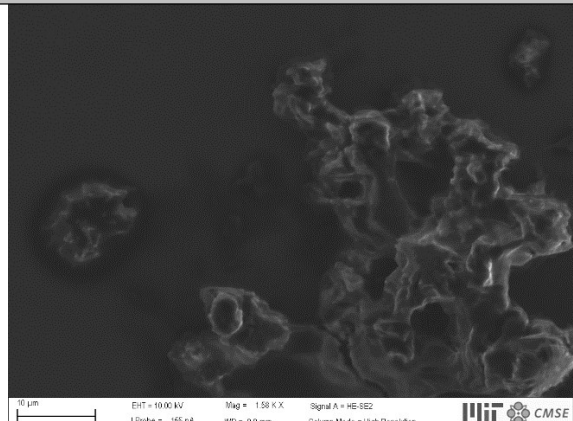
6-Form II spherical agglomerates



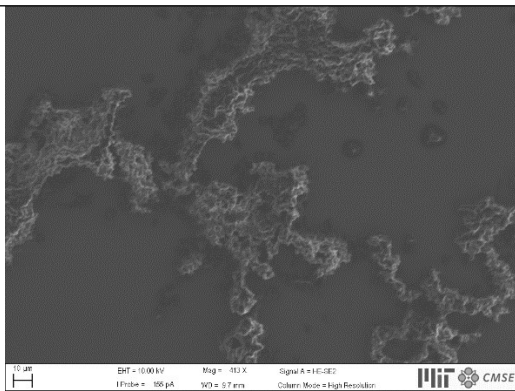
8-Form II spherical agglomerates



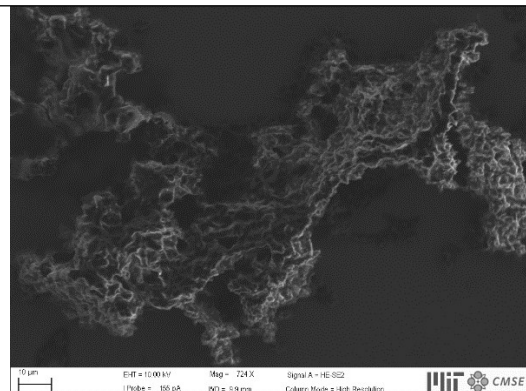
9-Form II spherical agglomerates



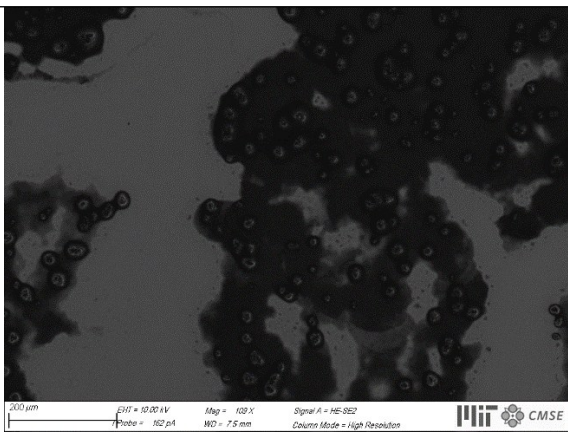
10-Form II spherical agglomerates



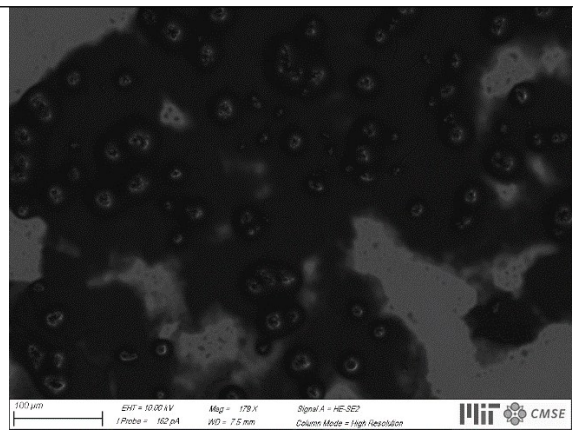
11-Form II spherical agglomerates



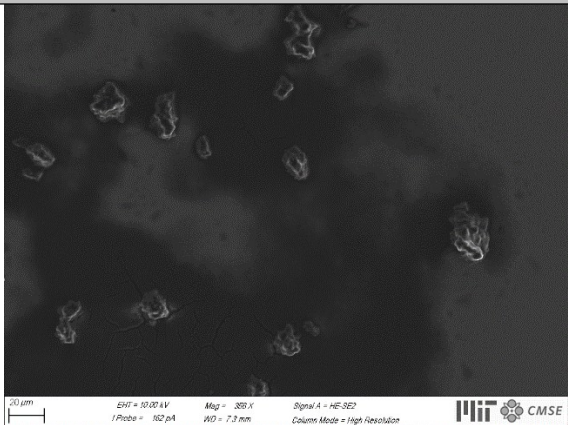
12-Form II spherical agglomerates



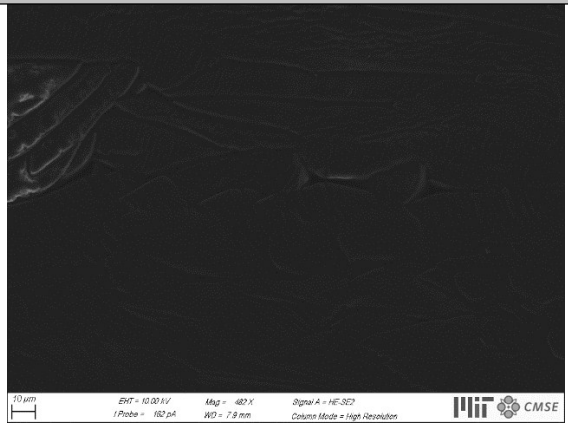
13-Form II spherical agglomerates



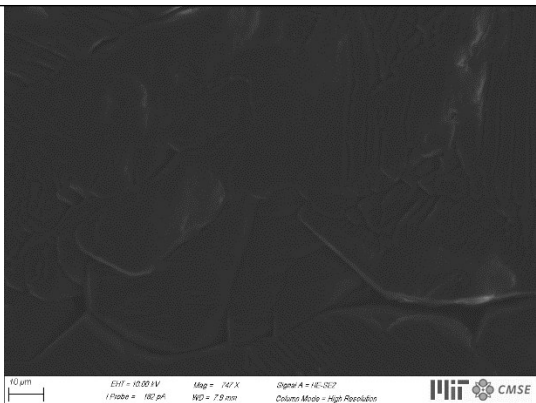
14-Form II spherical agglomerates



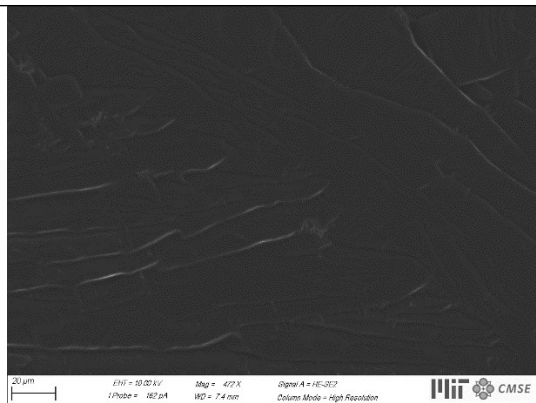
15-Form II spherical agglomerates



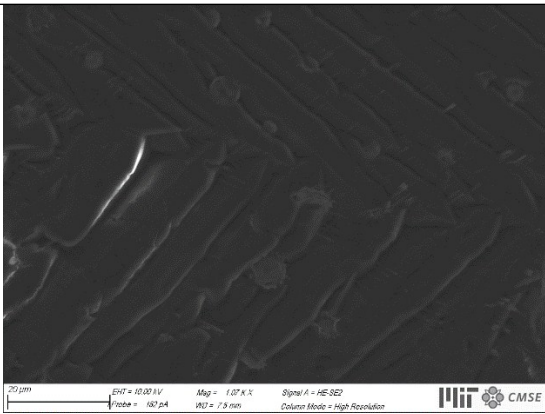
16-Form II 2D step growth surface



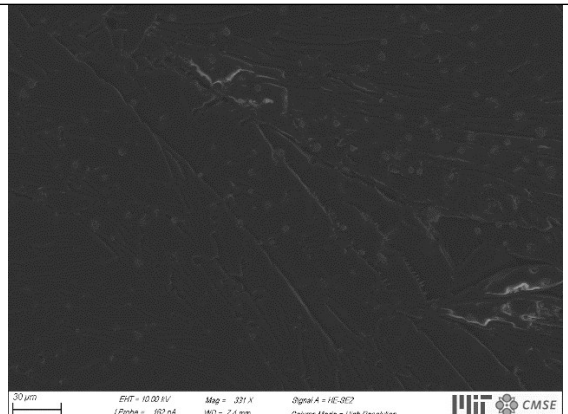
17-Form II 2D step growth surface



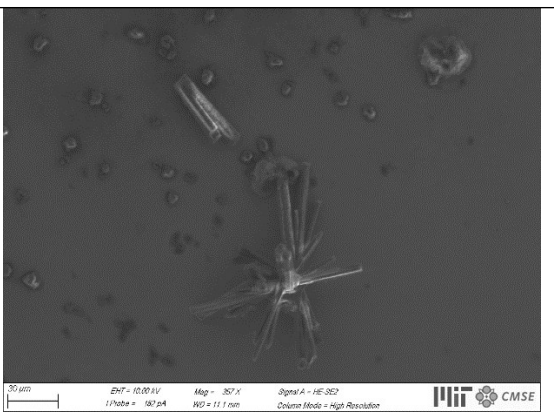
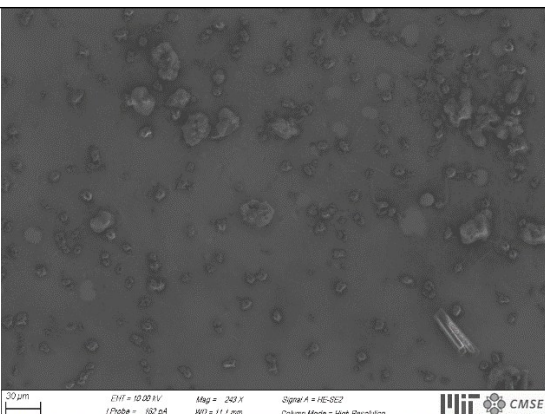
18-Form II 2D step growth surface



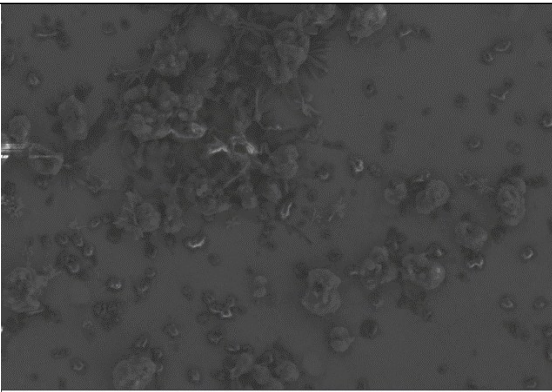
19-Form II 2D step growth surface and spherical agglomerates



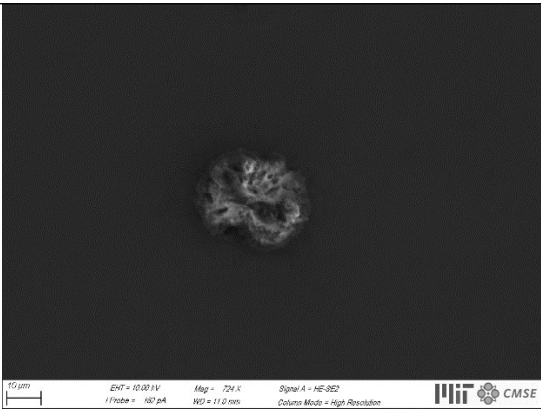
20-Form II 2D step growth surface and spherical agglomerates



21-Form II agglomerates and 1D needle crystals

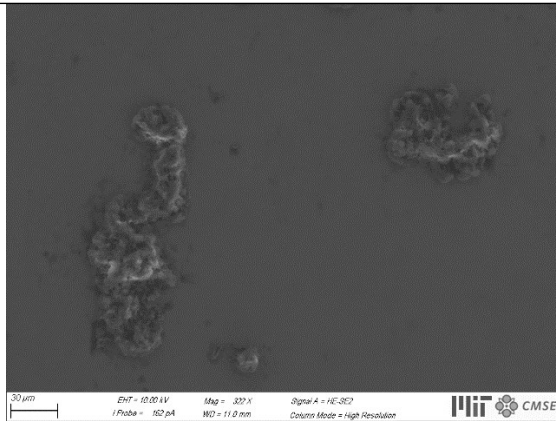


23-Form II 2D agglomerates and 1D needle crystals

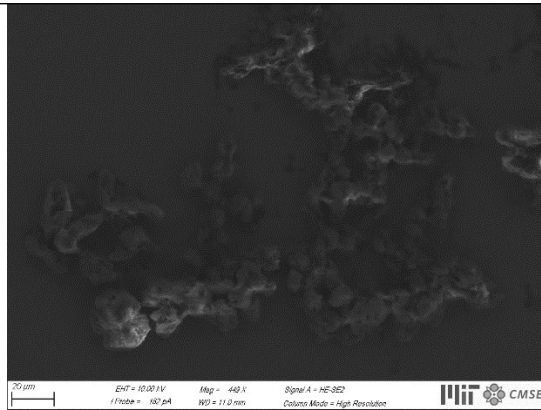


25-Form II agglomerates

22-Form II agglomerates and 1D needle crystals



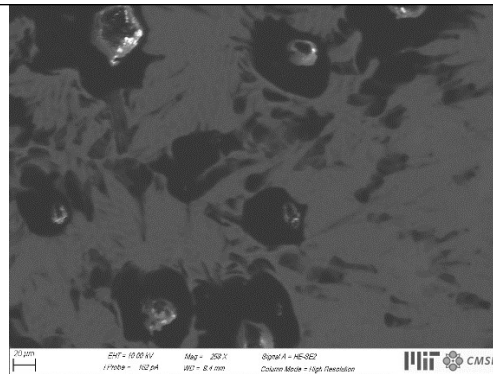
24-Form II agglomerates



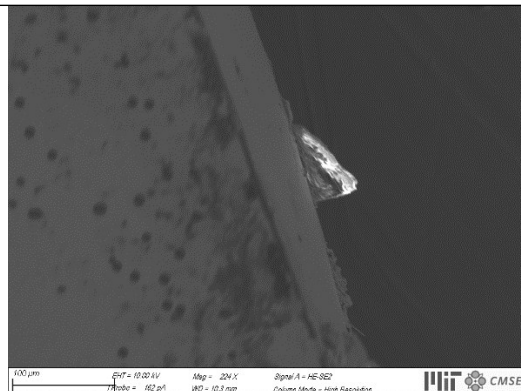
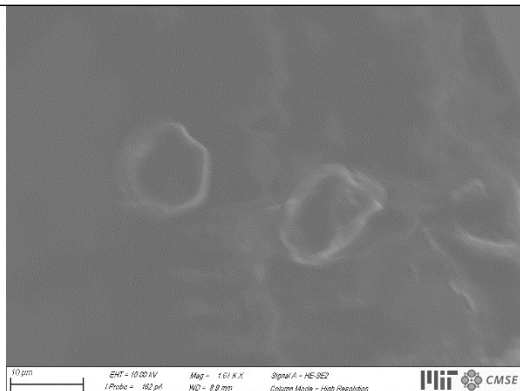
26-Form II agglomerates



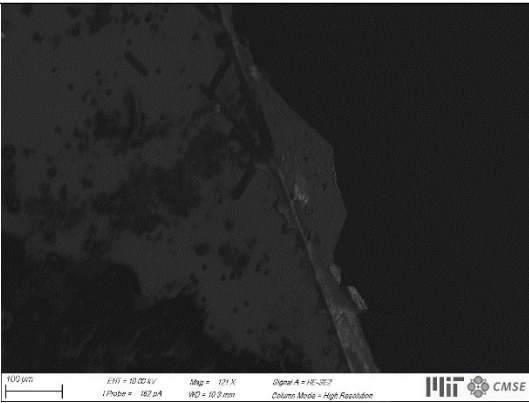
27-Form II 2D crystals



28-Form II 2D crystals

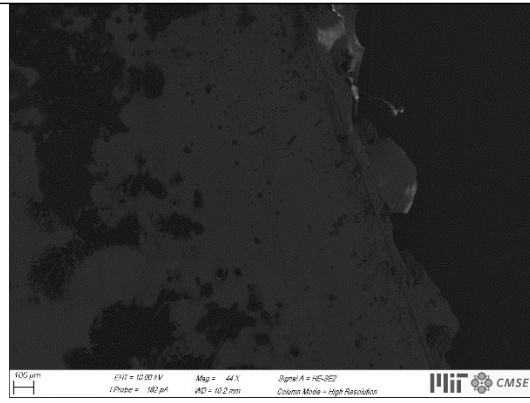


29-Form II 2D crystals

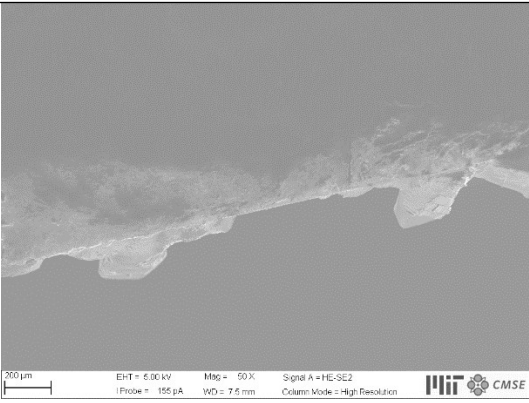


31-Form II 2D crystals at edge

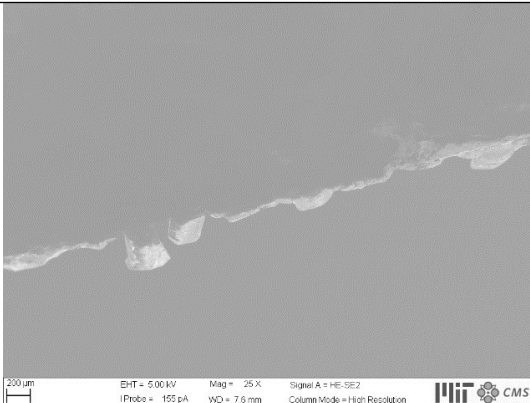
30-Form II 2D crystals at edge



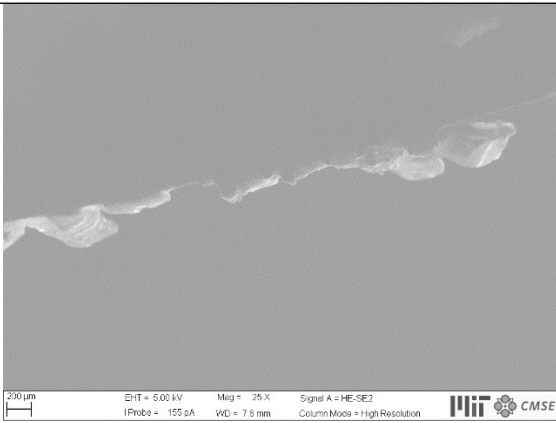
32-Form II 2D crystals at edge



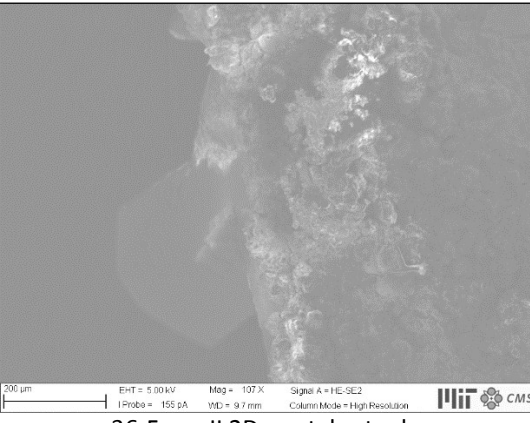
33-Form II 2D crystals at edge



34-Form II 2D crystals at edge



35-Form II 2D crystals at edge



36-Form II 2D crystals at edge

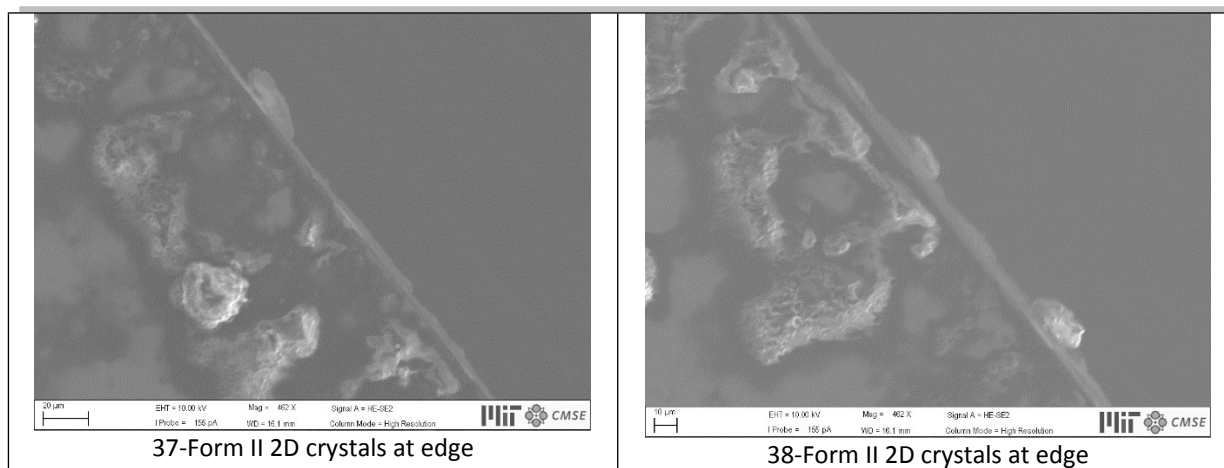


Figure S11. (a) APAP Form I dendrite growth and crystals block, prismatic growth on SURMOF surface SEM images. (b) APAP Form II different crystals and different surface and at edge of the substrate.

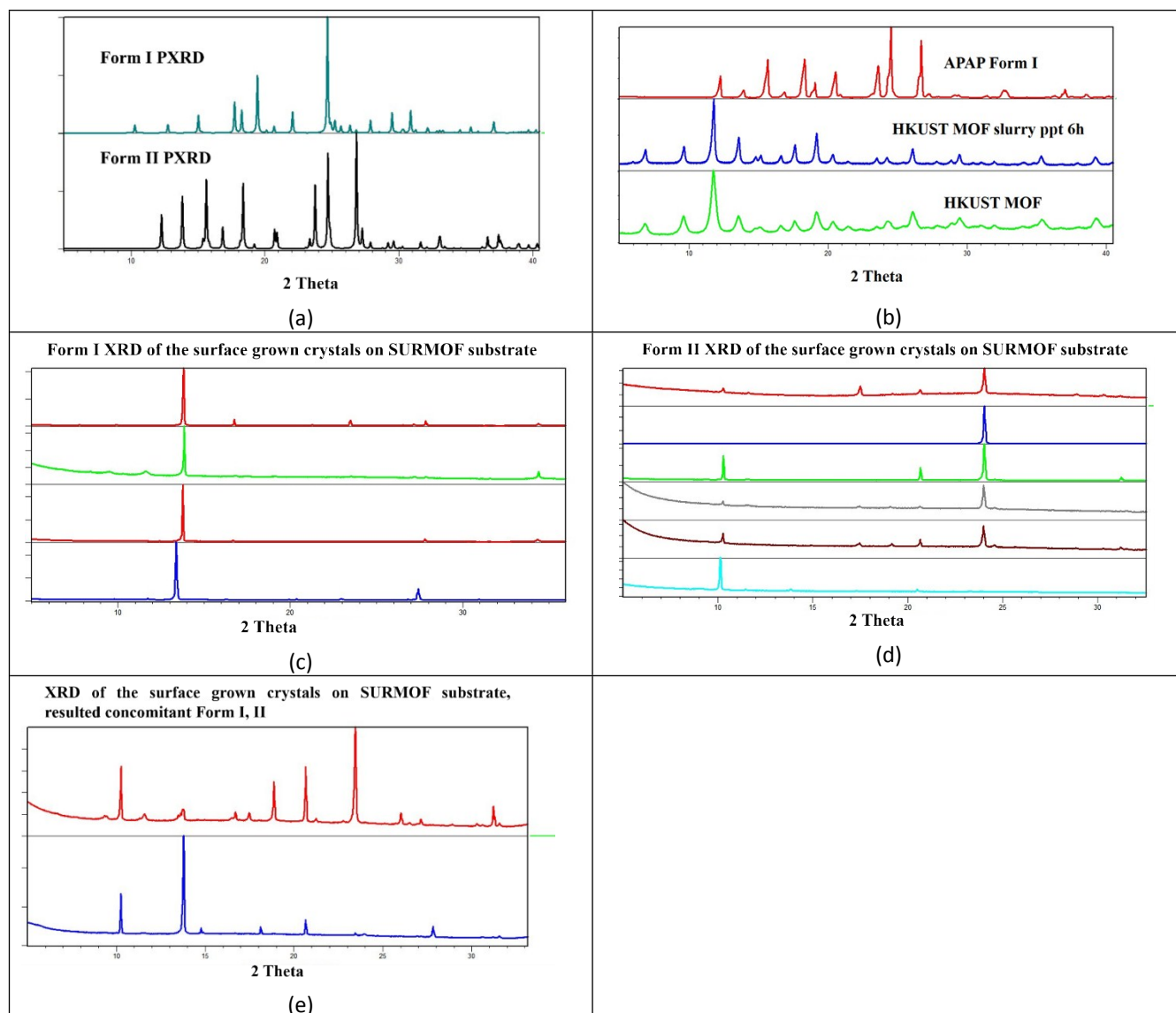
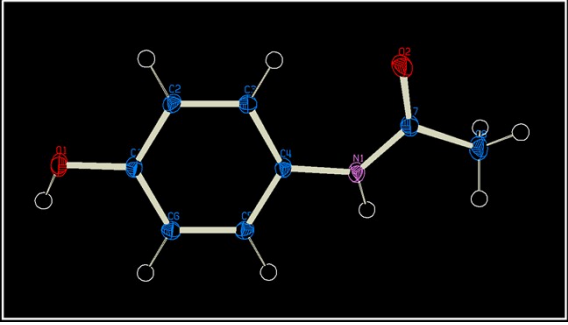


Figure S12. X-Ray diffraction study of the Form I and II.

Table S4. Crystallographic parameters of the Form II single crystal collected present study.

CCDC number	1814819
Chemical formula	C ₈ H ₉ NO ₂
Formula weight	151.16
Space group	Pbca
Temperature (K)	100
a (Å)	11.7678(7)
b (Å)	7.1966(5)
c (Å)	17.1615(11)
α (°)	90
β (°)	90
γ (°)	90
V (Å ³)	1453.38
D _{calc} , gcm ⁻³	1.382
Z	8
μ (mm ⁻¹)	0.10
No. of measured, independent, observed [I > 2σ(I)] reflections	47305, 2436, 2198
R _{int}	0.0386
R[F ² > 2σ(F ²)], wR(F ²), S	0.0471, 0.1394, 1.206
Goof	1.082
Diffractometer, Radiation type	Bruker Apex-II
	
ORTEP diagram of Form II at 50 % propability, plotted in PLATRON	

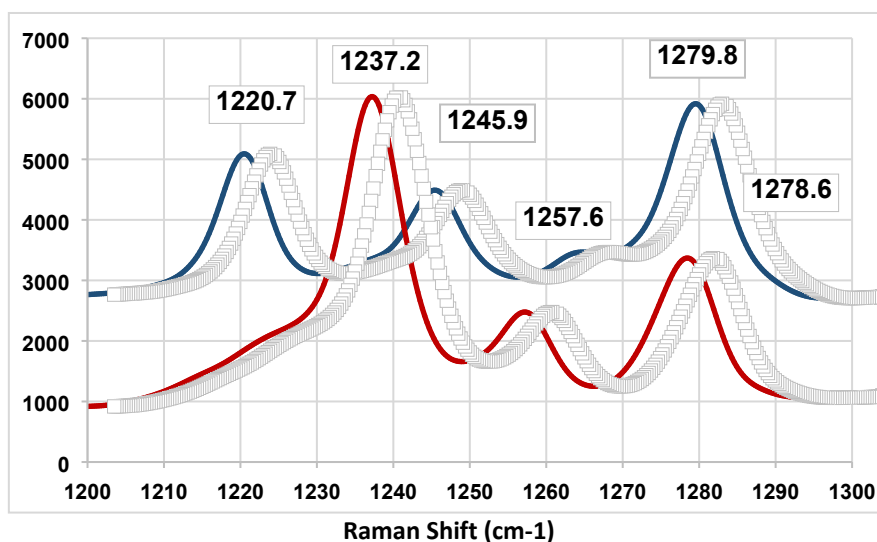


Figure S13. Raman comparison of the APAP Form I (Red) and II (blue).

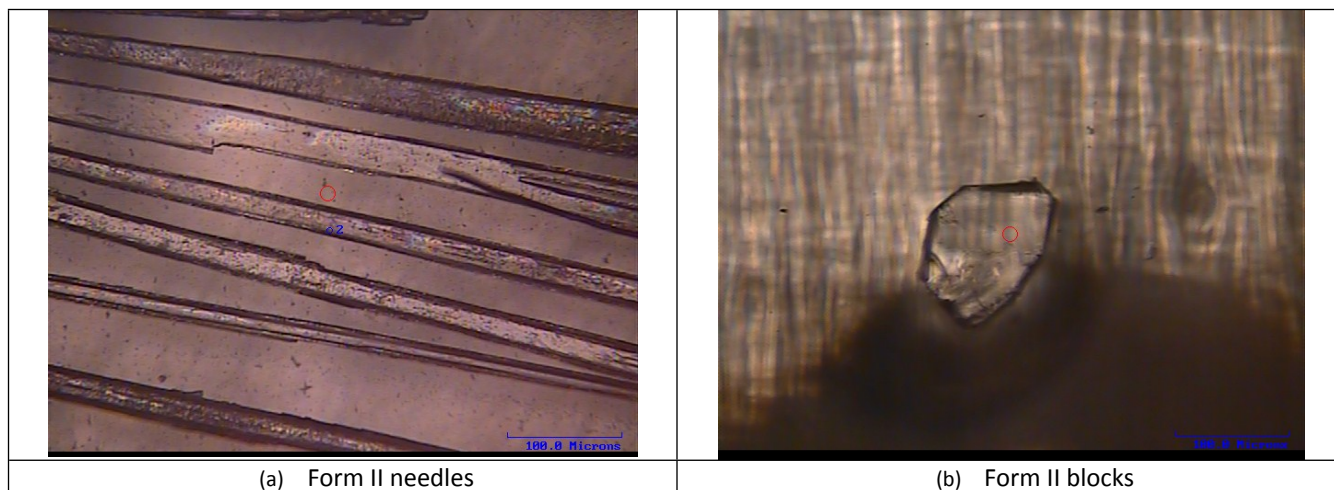


Figure S14. Optical microscope images of the of the APAP Form II (a) solvent crystallization seed with Form II with out substrate. (b) Form II with substrate.

References

- 1 G. M. Sheldrick, *Acta Cryst.* **2015**, *A71*, 3–8.
- 2 G. Nichols and C. S. Frampton, *J. of Pharm Sci.*, 1998, **87**, 684–692.
- 3 R. I. Ristic, S. Finnie, D. B. Sheen and J. N. Sherwood, *J. Phys. Chem. B.* 2001, **105**, 9057–9066.

